Progress in Understanding Degradation Mechanisms and Improving Stability in Organic Photovoltaics

*William R. Mateker and Michael D. McGehee**

Understanding the degradation mechanisms of organic photovoltaics is particularly important, as they tend to degrade faster than their inorganic counterparts, such as silicon and cadmium telluride. An overview is provided here of the main degradation mechanisms that researchers have identified so far that cause extrinsic degradation from oxygen and water, intrinsic degradation in the dark, and photo-induced burn-in. In addition, it provides methods for researchers to identify these mechanisms in new materials and device structures to screen them more quickly for promising long-term performance. These general strategies will likely be helpful in other photovoltaic technologies that suffer from insufficient stability, such as perovskite solar cells. Finally, the most promising lifetime results are highlighted and recommendations to improve long-term performance are made. To prevent degradation from oxygen and water for sufficiently long time periods, OPVs will likely need to be encapsulated by barrier materials with lower permeation rates of oxygen and water than typical flexible substrate materials. To improve stability at operating temperatures, materials will likely require glass transition temperatures above 100 °C. Methods to prevent photo-induced burn-in are least understood, but recent research indicates that using pure materials with dense and ordered film morphologies can reduce the burn-in effect.

1. Introduction

Organic photovoltaics (OPVs) represent an exciting class of photovoltaic materials.[1] OPV materials absorb light strongly, with absorption depths of only a few hundred nanometers. The materials can be solution-processed onto flexible substrates, enabling fast and inexpensive manufacturing processes.[2] Both the capital expense and energy payback period of OPVs are projected to be less than that of other photovoltaic products.[3–6] Device efficiency has increased rapidly due to improvements in both device and materials engineering. The world record OPV efficiency has reached 13.2%,[7] and many material combinations are above 10%.[8–13] By some estimates, devices could soon reach 15%[14] which could make OPVs attractive in some commercial applications.

To be commercially viable, an OPV must perform consistently throughout its lifetime. There is a high bar for any new product used in large-scale energy production, as established PV companies that employ materials such as crystalline silicon or cadmium telluride warranty their products for 25 years.[15] Even though it is estimated that OPVs might only need to retain performance for 10 years to become commercially competitive,[4,16] achieving that stability presents a significant challenge.

Performance loss in OPVs over time is widely observed. Across various studies, the degradation observed in OPVs falls into three general time regimes: an initial period of steep degradation that slows down with time, a period of relatively constant degradation that lasts for most of the solar cell's usable lifetime, and rapid and complete degradation that results in device failure (**Figure 1**, top). The initial period of steep degradation is typically referred to as "burn-in". The term itself is a reference to the commercial practice in electronic device manufacturing of a short thermal treatment before shipping to customers. Such a treatment slightly reduces the initial performance but ultimately enhances product stability; consumers receive a "burned-in" device that performs consistently through time. If the time duration of burn-in is short relative to the lifetime of a device, then efficiency loss during burn-in is conceptually similar to a loss in initial efficiency. Interestingly, and unfortunately, OPV burn-in tends to be more severe and protracted than in other electronic devices; during a time frame of several hundred, or even a thousand, hours, initial efficiency typically decreases by 10–50%. Like other electronic devices, once OPV burn-in ends the degradation rate becomes relatively constant and is typically much slower than burn-in. This regime marked by long, linear degradation is referred to as the "long-term" degradation period. At the "stabilized" long-term rate, it can take thousands or even tens of thousands of hours to reduce performance by another 20%. Degradation that results in complete device failure in just 10's of hours is categorized as "failure." Failure can occur during either the burn-in period or the long-term period.

In the present work, the underlying physical and chemical mechanisms that drive the different time regimes over which degradation occurs are discussed – burn-in, long-term, and failure. These mechanisms can be broadly grouped into three categories: extrinsic degradation caused by chemical reaction with water and oxygen, intrinsic degradation in the dark, and intrinsic photo-induced degradation.

Dr. W. R. Mateker, Prof. M. D. McGehee
476 Lomita Mall
Stanford, California 94305
E-mail: mmcgehee@stanford.edu

DOI: 10.1002/adma.201603940

Extrinsic degradation occurs when oxygen and water from the atmosphere are allowed to enter an OPV. Oxygen that enters the organic layers can react with the materials under illumination and cause them to bleach, or lose the ability to absorb light. Both oxygen and water are known to react with the low work function metals that are commonly used as buffer layers. Each of these mechanisms can be identified by rapid device failure and loss of active area. Encapsulation can significantly slow these mechanisms, though if the encapsulation fails at any time or if atmosphere permeates through the barrier layer, extrinsic degradation will persist.

Even perfectly encapsulated devices degrade intrinsically over time. Storing or heating solar cells in the dark and periodically measuring their performance is the typical way researchers identify dark degradation. Dark degradation usually results from molecular rearrangement in the absorber layer or organic buffer layers. On a short time scale, molecules segregate and rearrange at material interfaces, forming layers that can hinder charge extraction. Over longer time scales, the two materials of the bulk heterojunction (BHJ) layer can phase separate over large distances, reducing the BHJ's ability to create free carriers from absorbed photons.

Additional degradation mechanisms occur under illumination. OPVs, particularly those made with solution-processed materials, exhibit a photo-induced burn-in that takes the shape of exponential decay of efficiency. Interestingly, this photo-induced burn-in stops after several hundred hours and does not completely degrade the device. Total efficiency loss caused by burn-in usually ranges from 10–50%. Depending on the materials used to make a BHJ, the photo-induced burn-in primarily causes a loss of short-circuit current (J_{SC}) or open circuit voltage (V_{OC}). Photo-dimerization of the fullerene molecule, especially C60 and [6,6]-phenyl-C_{61}-butyric acid methyl ester (PCBM), is proven to be a key mechanism that leads to J_{SC} loss. While the underlying photo-chemical mechanism that causes V_{OC} loss is less clear, an increase in energetic disorder on the polymer material is suspected. It is particularly intriguing that this photo-induced burn-in ends without completely degrading the solar cell's efficiency, and several competing hypotheses attempt to account for both the kinetics of burn-in and why it stops. This photo-induced degradation behavior is particularly different than crystalline silicon, which is relatively stable under light, and necessitates extra testing protocol to evaluate OPV stability.

We also review the progress in improving the stability of OPVs and offer additional suggestions for future researchers. Perhaps most importantly, proper encapsulation can significantly reduce extrinsic degradation that causes rapid device failure and is necessary for long-term stability. Inverting the polarity of OPV devices and replacing low work function metals can improve solar cell shelf stability in air, but it cannot prevent material bleaching under illumination. Using materials with high glass transition temperatures improves the stability at elevated temperatures, and purification and fractionation of polymers are also shown to improve shelf and light stability of OPV devices. Dense, crystalline BHJ film morphologies can improve the photo-chemical stability of the semiconductor materials themselves. Switching from PCBM to $PC_{71}BM$ or to higher adduct fullerenes can eliminate the photo-dimerization that causes J_{SC} loss. It is possible that non-fullerene acceptor materials will also reduce photo-induced J_{SC} loss.

While much of the content in this review is specific to OPVs, the general methodology used to identify underlying degradation mechanisms can be extended to other thin film solar technologies. The chemical mechanisms in particular may be general to other electronic devices that use organic semiconductors, like organic light emitting diodes (OLEDs) or perovskite solar cells that use OPV materials like poly(3-hexylthiophene) (P3HT) and PCBM as buffer layers.[17–19]

Billy Mateker graduated with a PhD. in Materials Science and Engineering from Stanford University in 2016, where he studied the degradation of organic photovoltaics under Michael D. McGehee. He received his undergraduate degree from Georgia Institute of Technology. He enjoys the outdoors and exploring nature on foot, by bike, and jeep. Since graduating, he has worked in the financial industry but could be convinced to return to clean tech.

Michael D. McGehee is a Professor in the Materials Science and Engineering Department and a Senior Fellow of the Precourt Institute for Energy. His research interests are developing new materials for smart windows and solar cells. He received his undergraduate degree in physics from Princeton University and his PhD degree in Materials Science from the University of California at Santa Barbara, where he did research on polymer lasers in the lab of Nobel Laureate Alan Heeger.

2. Basic OPV Operation

An OPV device is comprised of an organic absorber layer sandwiched between two electrodes (**Figure 2**). In the simplest OPV, a transparent electrode, the absorber layer and a reflective electrode are sequentially deposited onto a substrate. Indium tin oxide (ITO) deposited onto glass represents the most common transparent electrode and substrate combination. The absorber layer of the most efficient OPVs is usually a blend of two

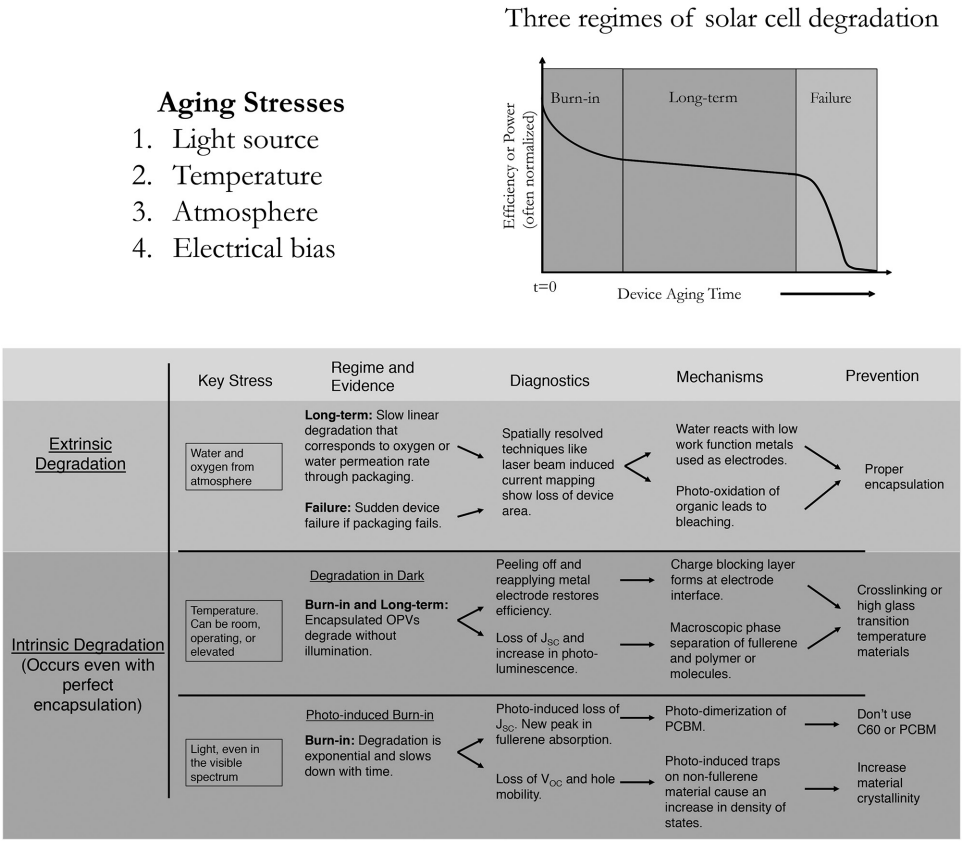

Figure 1. Top, left) Experimentalists must consider four main stressors when conducting long-term testing. Top, right) When OPV performance is tracked over time, there are typically three distinct degradation regimes, which are illustrated schematically. During burn-in, degradation is initially steep and slows down with time. In the long-term regime, degradation usually continues at a constant rate. Rapid and complete device degradation results in failure. Bottom) This chart summarizes the main degradation mechanisms observed by researchers.

materials that form an interpenetrating bulk-heterojunction[20] throughout the entire thickness of the film. One of the BHJ materials is almost always a fullerene,[21] while the other can be a polymer or another molecule.[22–25] A reflective metal, deposited last, allows any light not absorbed by the absorber layer to pass through the device a second time. Buffer layers can be added between the absorber layer and electrodes and are often employed to set an electric field across the absorber layer or preferentially collect holes or electrons at the proper electrode.[26] These buffer layers can be low work function metals, metal oxides or other organic materials. More detailed reviews of BHJ solar cell operation are available.[1,3,27–29]

3. Experimental Techniques for Studying Degradation

Photovoltaics experience four main stressors: light from the solar spectrum, increased temperature, exposure to atmosphere, and electrical bias. Each of these stressors can cause organic materials to degrade, and degradation is compounded when multiple stressors are combined. The only way to test the long-term performance of a solar cell in true real-world operating conditions is outdoor testing. Outdoor testing can be an effective way of identifying real-world failure mechanisms,[30–32] but because conditions are not controlled, it is difficult to assign degradation mechanisms to a specific stress or even combination of stressors. To resolve this issue and enable the mechanisms of degradation to be scientifically studied, researchers use a combination of artificial light, temperature control, encapsulation or atmospheric control, and power electronics

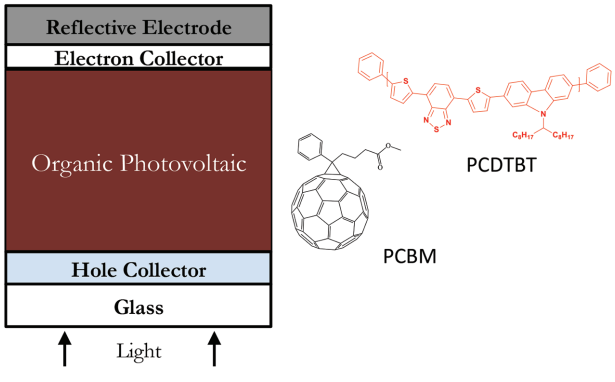

Figure 2. Left) A schematic of an OPV device in the standard architecture. Switching the electron and hole collector inverts the polarity. Right) A schematic of PCBM, one of the most common materials used in high efficiency OPVs, and poly[N-9′-heptadecanyl-2,7-carbazole-alt-5,5-(4′,7′-di-2-thienyl-2′,l,3′-benzothiadiazole) (PCDTBT), a well-studied polymer.

to monitor the long-term performance of solar cells in a controlled environment.

Historically, the conditions used to simulate each stress have varied among OPV researchers. When choosing a source of artificial sunlight, researchers must consider the spectrum match to AM1.5G, energy usage and incidental heating to the lab, and the lifetime of the light source itself. Many researchers use xenon[33,34] and metal halide[35] lamps, because their spectra match AM1.5G relatively well across all wavelengths, especially when filters are applied. However, the usable lifetime of these lamps extends to only 1500–2000 hours, which is shorter than the duration of some experiments.[36] Some researchers instead use sulfur plasma lamps,[37] which last considerably longer and are more energy efficient than xenon arc lamps. While their spectra matches AM1.5G well in the visible wavelengths, it contains little UV radiation, which can impact the long-term performance.[38] Illumination also increases the temperature of the solar cells, and the amount of heating can vary with light source. To reduce solar cell heating, some researchers have begun using white light emitting diodes (LEDs).[39]

Researchers also use temperature controlling apparati to set a specific temperature, usually in the range from 50–65 °C, which corresponds to the higher end of operating temperature range.[40] To independently examine the degradation effects of illumination and increased temperature, some solar cells are shaded and aged at the same temperature of illuminated cells, or similarly aged on a hotplate kept in the dark. To protect OPVs from oxygen and water, many researchers encapsulate the solar cells. Both flexible barriers[41–43] and glass-on-glass[37,44–46] encapsulation methods are used. For even greater control, some researchers use sealed chambers that can vary and monitor the oxygen and water content of the atmosphere.[36,38,47] Finally, researchers must consider the electrical bias at which to age OPVs, as bias condition can impact degradation. Power electronics keep an operating rooftop solar module at or near its maximum power point. To reproduce this real-world bias condition, some researchers use custom electronics to monitor and adjust OPVs to their maximum power point for the duration of a long-term test.[48] If the maximum power point information is stored, it doubles as a characterization tool. However, it is cheaper to simply illuminate solar cells at their open or short circuit current bias conditions, and periodically test their performance using one source-measure unit and a multiplexer.[49]

To increase reproducibility across different labs, an experimental protocol has been outlined by the International Summits on OPV Stability (ISOS).[50] The guideline presented by ISOS has general testing categories that include dark, outdoor, laboratory weathering, thermal cycling, and solar-thermal-humidity cycling tests. Within each category there is a basic, intermediate, and advanced level of testing. The required light source and spectra, temperature control, atmospheric conditions, electrical bias and monitoring are listed for each level. Round-robin tests among different labs demonstrate that strict reproducibility among labs is difficult.[51–54] The ISOS protocol was recently reviewed and compared to other thin film solar testing protocol in greater detail.[55]

It is helpful to define a performance metric that describes the "lifetime" of an OPV, and a common definition exists in two flavors. Under the first, the relative performance over time is indexed to the initial performance, and the lifetime is the time duration to reach some relative percent of initial performance. The most common relative values used are 80% and 50%, and the lifetimes corresponding to those values are referred to as T_{80} or T_{50}. Using this working definition, most OPV solar cells reach the end of their usable lifetimes during burn-in, and lifetimes are only hundreds of hours. Under the second definition, burn-in is viewed as conceptually similar to a reduction of initial performance, and the relative efficiency through time is indexed to the efficiency at the end of burn-in. This is referred to as the "stabilized lifetime". Stabilized lifetimes, or T_{S80} or T_{S50}, typically correspond to thousands to even tens of thousands of hours. To put these figures into context, a solar cell deployed in the state of California is exposed to an average solar flux that corresponds to 5.5 h of direct sunlight per day, or roughly 2000 h per year. Thus, stabilized lifetimes are typically several years. Lifetimes longer than a few thousand hours are usually extrapolated, as they correspond to months of continuous illumination. To date, the longest extrapolated T_{S80} is over 40 000 h, which in the state of California equates to a lifetime of approximately 20 years.[36]

4. Extrinsic Degradation

Extrinsic degradation occurs when OPVs are aged in ambient conditions, either in the dark or under illumination, such that oxygen and water can permeate into the device. It is evident by the growth of "dead zones", or areas of the solar cell that no longer produce photocurrent. Dead zones are linked to oxygen and water diffusion by spatially resolved characterization techniques, such as laser beam induced current (LBIC) mapping, of degraded solar cells that show dead zone growth around pinholes in the metal electrodes or along electrode edges[56–58] (**Figure 3**a). Indeed, isotopic labeling of oxygen atoms in water and oxygen shows that concentrations of both molecules increase in unencapsulated OPVs over time.[59] Researchers have directly elucidated the underlying degradation mechanisms related to oxygen and water permeation, as well as ways to improve stability. The two most prevalent extrinsic degradation mechanisms are oxidation of the metal electrodes and associated buffer layers, and photo-oxidative loss of absorption, or bleaching, of the semiconductor materials. Eliminating low work function metals from the device stack can slow oxidation of the metal electrodes or buffer layers. Eliminating solubilizing side chains, forming dense, crystalline film morphologies, and blending with fullerenes can slow photo-oxidative bleaching of the semiconductor materials.

4.1. Electrode Degradation

Electrodes on OPVs serve three key functions – to set an electric field across the absorber layer to drive electrons and holes to the appropriate contact, to provide a proper energy level to selectively extract the electrons or holes that reach the contact, and, like all PV technologies, to provide a low resistance pathway to laterally transport charge out of the device. At least one of the electrodes must be transparent to allow light into

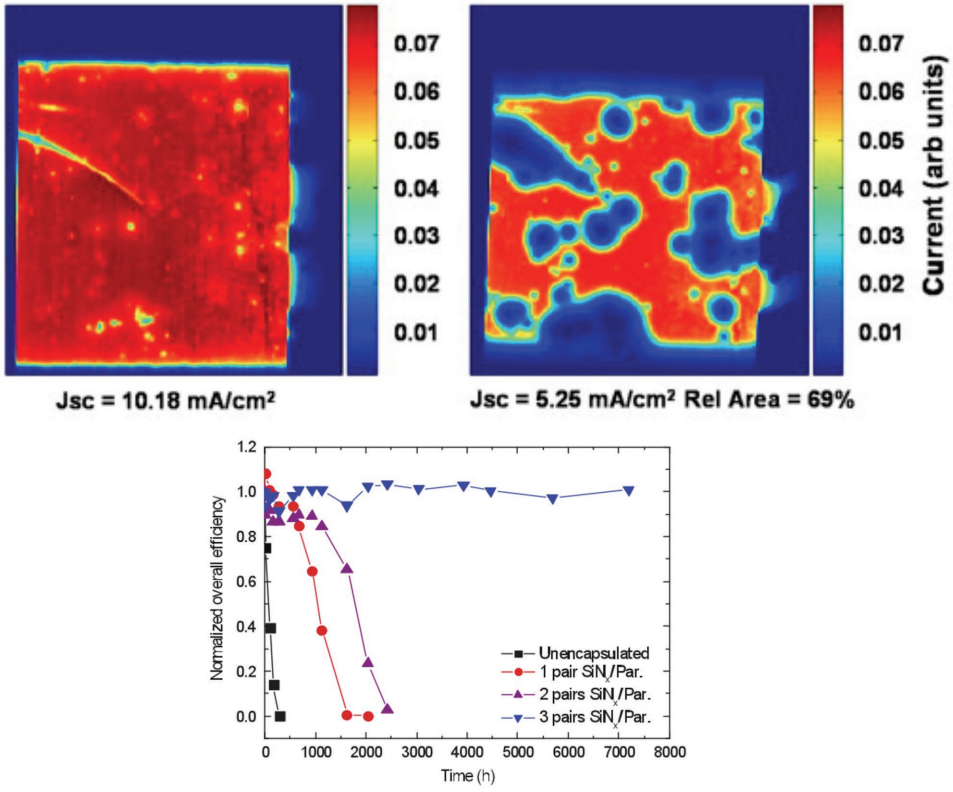

Figure 3. Top) Laser beam induced current (LBIC) map of a solar cell before (left) and after (right) prolonged illumination in ambient conditions. In the degraded solar cell, dead zones clearly form around pinhole defects and there is significant ingress around the edges of the device. Reproduced with permission.[56] Copyright 2011, Elsevier. Bottom) OPVs are periodically measured under dark storage conditions with an increasing level of encapsulation. Unencapsulated solar cells fail within 10's of hours. One layer of the organic-inorganic encapsulate slows failure for 1000 h, two layers slows failure for nearly 2000 h, and three layers slows failure for more than 7000 h. Reproduced with permission.[60] Copyright 2012, Elsevier.

the absorber layer. Because OPVs do not usually absorb all the light in a single pass, the other electrode is usually reflective to increase the distribution of light in the absorber layer. Low work function metals evaporated on top of the absorber layer, such as calcium and aluminum, were first used to efficiently extract photo-excited electrons and maximize the V_{OC} of the solar cells, as well as reflect light back into the absorber layer.[61,62] By convention, this polarity (extracting electrons at the metal, extracting holes at the transparent electrode) is referred to as "standard," while the opposite is referred to as "inverted."

Low work function metals are well known to oxidize when exposed to atmosphere, particularly to water, without exposure to light.[63] Oxidation alters the work function or the conductivity of the layer, both of which cause a reduction in performance. Metal electrode degradation from water, in the form of dark spot growth, was first observed in OLEDs, which also incorporate low work function metals as electrode materials in their device stacks.[64–67] Research on unencapsulated OPVs shows that water diffusion into electrode pinholes and at the edges of the solar cell cause dead zones to grow, even without illumination.[57] A way to substantially improve shelf stability of unencapsulated devices is to remove low work function metals from the device stack completely. This can be accomplished using an inverted architecture, where electrons are collected at the transparent electrode and holes are collected at the reflective one.[68] Indeed, in studies that compare the shelf stability of unencapsulated standard and inverted architecture OPVs, the stability of inverted devices is dramatically improved.[69,70]

4.2. Absorber Layer Bleaching

OPV materials are well known to degrade in the presence of oxygen and light.[71,72] Photo-oxidation causes organic films to lose optical density (**Figure 4**). Researchers most commonly track the extent of degradation by measuring the loss of absorption in OPV films as a function of illumination time. Bleaching of the film's absorption is typically observed to occur on a timescale of seconds to hours under one-sun intensities. Chemical analysis by means of infrared spectroscopy of the degradation products of a variety of polymers, including PPV's,[75,76] P3HT,[73,77–80] PCDTBT,[81,82] PTB7,[83,84] PBDTTPD,[85] Si-PCPDTBT[86] and others[87] shows a loss of conjugated bonds and a growth of carbonyl, ester, and alkoxy bonds, indicating the materials react with oxygen.

The chemical mechanism that leads to photooxidation is generally thought to proceed via a free-radical reaction.[72] The presence of free radicals in aged polymer films can be detected by electron spin resonance (ESR), and the concentration of free radicals is observed to increase with illumination time.[88] The

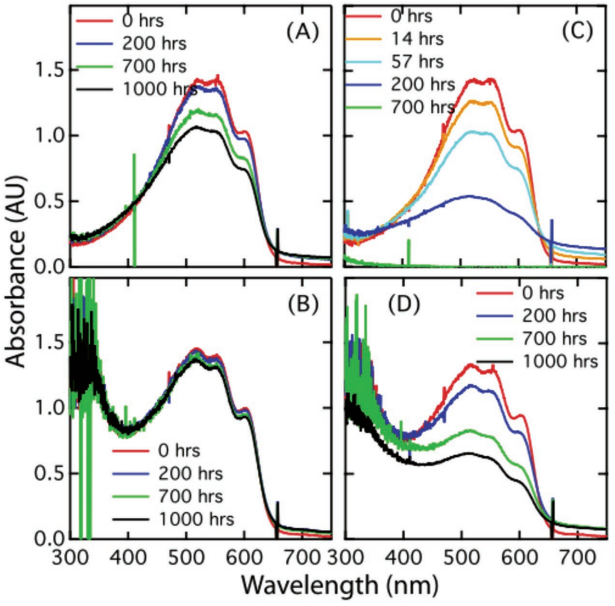

Figure 4. Films of P3HT (A), and P3HT blended with PCBM (B) that are stored in the dark retain much of their absorption features. Under illumination, a film of P3HT (C) loses most of its ability to absorb light after 200 h and is completely bleached in 700 h. A P3HT film blended with PCBM (D) and illuminated retains its absorption features for at least 1000 h in the same conditions. Reproduced with permission.[73] Copyright 2010, Wiley.

general steps, which consist of initiation, propagation, and termination, of such a reaction are outlined at the top of **Figure 5**. Generally, initiation occurs when a bond breaks. Once a free-radical is formed, it can propagate through the film via diffusion or reaction. During propagation, scission of the conjugated bonds ensues, which is the direct mechanism for absorption loss. Termination occurs when two free-radicals meet and recombine. In OPV materials, free-radical reaction is often initiated when a hydrogen atom is abstracted from the alpha carbon of a side chain. After this initiation step, the free radicals must propagate through the film for the reaction to proceed. Propagation is accelerated in the presence of oxygen, as oxygen can readily diffuse throughout the film. A specific free-radical reaction pathway is shown for PCDTBT. The initial free radical on PCDTBT is formed at the carbon adjacent to the nitrogen on the carbazole unit. In the case of PCDTBT, recombination of free-radicals on adjacent backbones and side chains results in crosslinking of the polymer film, which has been observed in films aged in the absence of oxygen. A general method for improving the photostability of solution-processed polymers is to remove the polymer's side chains, which commonly act as free-radical reaction initiation points.[89]

Though the nature of the chemical bonding among OPV materials is relatively similar, the rate at which specific OPV materials bleach can vary substantially.[90,91] In one study, different OPV materials bleach at rates that span over five orders of magnitude.[92] Film morphology in OPV materials can vary from completely amorphous to semi-crystalline, and the film morphology is found to play an important role in the photooxidative stability observed in OPV materials. In comparisons between materials that can be cast in both amorphous and crystalline film morphologies, the crystalline films are always observed to be more stable.[79,91,92] Film density is also correlated to stability; denser films tend to be more stable to photooxidation, possibly because the molecules are more confined and oxygen is less able to diffuse to reaction sites.[92] The relationship between film morphology and photooxidative stability is not unique to OPV materials - morphology and film density is also observed to strongly affect the reactivity of molecular crystals and organic pigments. In fact, in many such systems the molecular arrangement and the physical constraints imposed in the solid state are found to have a greater impact on a material's photostability than the innate reactivity of the materials itself.[93–97] Increasing film density is one method to improve the stability of organic pigments.

As the most efficient OPV devices contain both a polymer (or small molecule) and a fullerene, researchers have also investigated the stability of blend films. It is generally found that mixing a polymer with the fullerene PCBM improves the photooxidative stability.[73,98–100] The stabilizing effect of PCBM is shown in Figure 4. After 200 h of illumination, a film of neat P3HT is almost completely bleached. A P3HT film blended with PCBM, however, retains a much of its optical density after 1000 h of illumination.[73] PCBM likely provides a stabilizing effect to photooxidation by several mechanisms. First, ultrafast electron transfer from the polymer to the fullerene quenches the excited state of the polymer.[101] Not only does this mechanism remove the excited electron from the polymer, but also competes with electron transfer from the polymer to form O_2^-, which may cause further degradation of the film.[100] The formation of O_2^- via electron transfer is proposed to occur when fullerenes with lower electron affinity are used instead of PCBM, and can accelerate the degradation of the polymer.[100] Second, fullerenes are proposed to act as free radical scavengers in thin films.[102] Fullerene cages are thought to be able to trap upwards of six to eight free radicals.

4.3. Preventing Extrinsic Degradation Mechanisms

Both electrode oxidation and absorber layer bleaching occur rapidly, and extrinsic degradation is the mechanism typically responsible for the failure regime observed by researchers in OPVs. Reports on the storage and light stability of unencapsulated OPVs observe rapid device failure and measure T_{80} and T_{50} lifetimes in only minutes to hours.[103–105] From work on organic light emitting diodes, encapsulation designed to prevent oxygen and water permeation is well known to improve stability.[64,65] Encapsulation of OPVs with flexible plastic barrier materials results in lifetimes approaching 1000 h,[41,42,106,107] while encapsulation with flexible organic-inorganic barrier films[108] or glass-on-glass further improves observed lifetimes to several thousands of hours.[35,37,44,109] It is important to note that protection from a permeation barrier is not always permanent. With some barrier materials, there is an induction period, or lag time, where no water or oxygen reaches the inside of the package.[110–112] During this lag time, the water or oxygen diffuses through the thickness of the barrier. To further extend the lag time before rapid degradation, many OLED devices add a

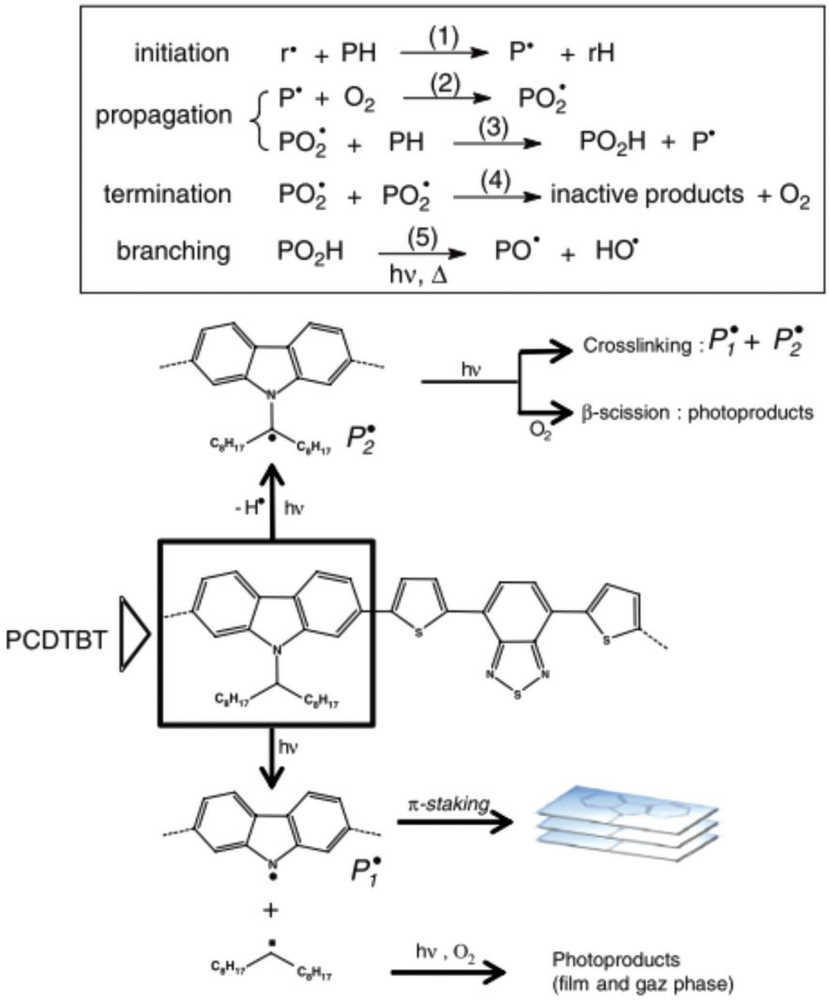

Figure 5. Top) In general, a chemical reaction that proceeds via a free-radical mechanism has three steps: initiation, propagation, and termination. Peroxyradicals may also branch under illumination. Reproduced with permission.[74] Copyright 2014, Wiley. Bottom) A schematic of the proposed degradation pathway of PCDTBT. In the initiation step of the reaction, a free radical is formed after illumination on the carbon atom of the side chain adjacent to the nitrogen of the carbazole unit. Reproduced with permission.[74] Copyright 2014, Wiley.

getter material to preferentially react with water or oxygen.[65] However, once atmosphere diffuses through the thickness and the getter material is completely reacted, a steady state permeation rate to the device ensues. Thus, the encapsulate will only protect the solar cells for a period of time before rapid device failure occurs (Figure 3b).[60,109] In essentially perfect encapsulation, when PCDTBT:$PC_{71}BM$ BHJ solar cells are aged in an environmental chamber that keeps oxygen and water levels below 0.1 ppm, a lifetime of 40 000 h, which corresponds to an equivalent of 20 years in the state of California, is observed (**Figure 6**).[36] This observation is particularly encouraging, as an organic material's stability under repeated photo-excitation, even in perfect conditions, is not assumed. It also implies that, if the quality of encapsulation is high enough, OPV's can in fact be long-term stable.

Researchers have attempted to estimate the quality of encapsulation necessary for such stable long-term performance. An upper bound on the water vapor permeation rate to sufficiently protect low work function metals in OLED devices has been made, and the conclusions reached apply to OPVs. Based on an assumption that the limit on the lifetime of an OLED is oxidation of its electrode (likewise, for OPV), Burrows estimates that the upper limit for water permeation rate of an adequate barrier is less than 10^{-5} g/m^2/day.[113] A similar estimate is made for the upper bound of the oxygen permeation rate through a barrier to protect the absorber layer from photo-oxidative bleaching.[92] Such rates are three to four orders of magnitude lower than the water permeation rate of untreated, flexible plastic substrate materials like polyethylene naphthalate and polyimides.[114] Thus, to achieve a shelf stability of 25 years, any OPV device that employs a low work function metal as an electrode necessitates glass-on-glass encapsulation techniques. If a flexible substrate is desired, the device must be packaged on both sides with a flexible barrier material with a sufficiently low water permeation rate, and research into reducing the cost of flexible barrier materials could improve the commercial viability of OPVs.[115–117]

4.4. Mechanical Degradation Mechanisms

In addition to the chemical reactivity of the component materials, to successfully prevent extrinsic degradation the mechanical integrity of the entire device stack must be considered.[118,119] OPVs are composed of multiple thin films, and encapsulation failure by delamination of these layers is observed in OPVs, particularly in flexible OPVs under temperature cycling.[58,120,121] Delamination can occur in two ways – when it occurs at the interface between two layers, it is referred to as adhesive failure, and when it occurs within one layer, it is referred to as cohesive failure.[122,123] The fracture energy (G_c), or the critical energy required to drive adhesion or cohesion processes, is measured in BHJ solar cells to be between 1 and 5 Jm^{-2}, which is relatively low compared to other thin film materials.[123,124] Adhesion and cohesion are observed to occur at or through areas of high PCBM concentration, and PCBM is identified as the mechanically weakest component in BHJ solar cells.[123–127] The fracture energy can be increased with higher molecular weight materials,[128] thermal treatments,[122,124,125] and choice of buffer layer material.[124]

5. Intrinsic Degradation

Proper encapsulation can exclude extrinsic degradation by reducing or eliminating the stressors caused by atmosphere,

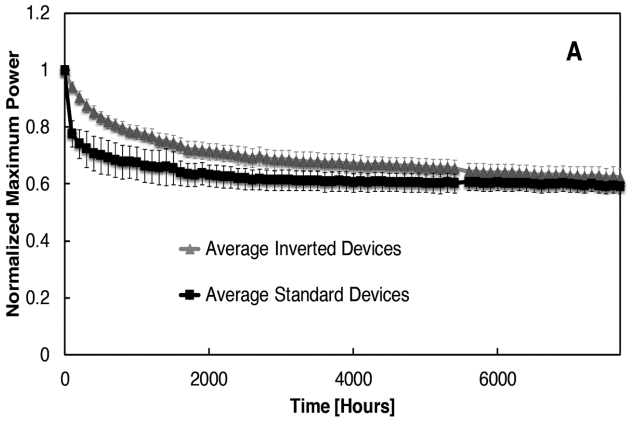

Figure 6. The normalized maximum power of PCDTBT:$PC_{71}BM$ solar cells aged in an environmental chamber is plotted against illumination time. Burn-in degradation reduces initial performance by nearly 40% over the first several thousand hours. Once burn-in ends, the solar cells are relatively stable and T_{80S} is extrapolated to greater than 40 000 h hours, which corresponds to an equivalent of 20 years in the state of California. Reproduced with permission.[36] Copyright 2015, American Chemical Society.

but it does not ensure OPV stability. Light and heat can provide sufficient stress to induce degradation. In long-term stability studies of encapsulated OPVs[35,37,44,46,109,129] and devices aged in environmental chambers,[36,47] both burn-in and long-term degradation are observed, as seen in Figure 6. Intrinsic degradation mechanisms can be grouped into two broad categories – degradation that occurs in the dark, and degradation that is caused by interaction with light. Dark degradation typically involves the movement of materials in the film, while light-induced degradation is caused by photo-chemical reactions that take place in the absorber layer. The following sections review degradations mechanisms that are observed in OPVs protected from atmospheric water and oxygen either by storage in an environment with a controlled atmosphere or encapsulation.

5.1. Degradation in the Dark

Researchers typically track dark degradation at three testing conditions – room temperature, solar cell operating temperature (between room temperature and 60 °C or so), and "accelerated conditions" corresponding to temperatures that exceed operating condition. When assessing the effects of dark degradation, solar cells are covered to reduce any effect of illumination and stored on a shelf or hotplate at the chosen temperature. The degradation of the OPVs is tracked by periodic current–voltage measurements under normal 1-sun testing conditions. Degradation that occurs when encapsulated OPVs are kept in the dark is widely observed.[130–135] Both the rate of degradation and the temperature at which degradation begins varies among material systems.[136] Some, such as PBDTTPD:PCBM and MDMO-PPV:PCBM BHJs, lose 10–20% of initial efficiency within a day, even when stored at room temperature.[129,137] Other systems, such as PCDTBT:$PC_{71}BM$ and PTzNTz:$PC_{71}BM$, are completely stable at operating temperatures and only begin to degrade when temperatures exceed 120 °C.[138–140]

The temperature at which solar cells begin to degrade is closely related to the glass transition temperature (T_g) of the component materials, with degradation beginning at temperatures above the lowest T_g.[133,138,141–144] For example, when the thermal stability of polymer:fullerene BHJs that use PPVs with high and low T_g's are directly compared, solar cells made from the low T_g PPV degrade at room temperature while the high T_g (138 °C) PPV solar cells do not.[141] In another study, the T_g of P3HT is measured to be 56 °C. P3HT:PCBM solar cells are stable when aged in the dark at 27, 37, and 47 °C but begin to degrade once the temperature reaches 57 °C (**Figure 7**).[138] In the same study, the T_g of PCDTBT is measured to be 135 °C, and PCDTBT:$PC_{71}BM$ solar cells are stable in the dark up to 127 °C. At temperatures above T_g, the polymer chains and molecules are able to move around in the films, and degradation is linked to their rearrangement. Crystallization of organic small molecules used as electrode buffer layers can also cause OPV

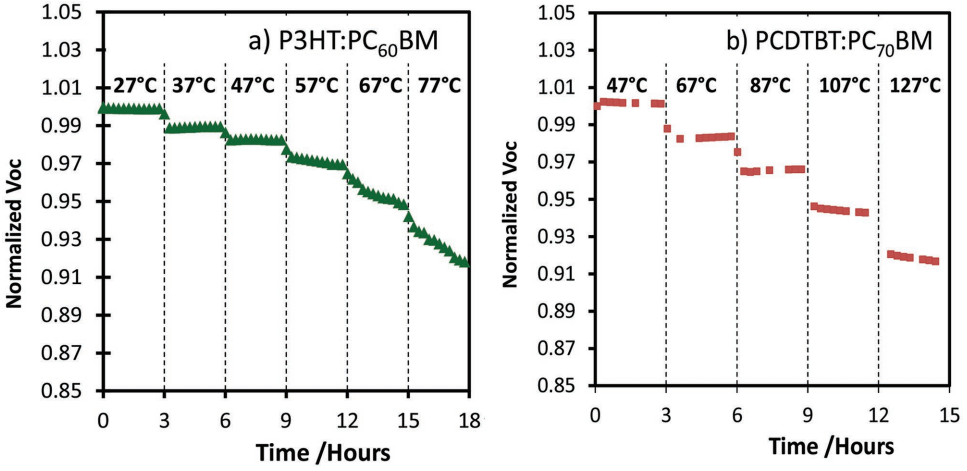

Figure 7. In polymer:fullerene solar cells, dark degradation is found to begin near the glass transition temperature (T_g) of the polymer. The T_g of P3HT is measured at 56 C, while PCDTBT's is 135 C. When solar cells are kept in the dark and periodically measured, their V_{OC} begins to degrade as a function of time near or above the T_g. Reproduced with permission.[138] Copyright 2014, Wiley.

degradation. When solar cells using Bphen are aged at 50 °C, crystallization of the Bphen causes the layer to crack and allows the metal to penetrate the active layer, leading to pin holes and shunting pathways.[145]

When OPVs are aged at temperatures above T_g, both interfacial and bulk mechanisms that lead to dark degradation have been identified. Peeling off the metal electrode with tape and re-evaporating a new metal electrode is one method used to isolate degradation mechanisms to the interface between the absorber layer and the evaporated metal;[33,39,137,138,146] if re-evaporating a new electrode on a degraded solar cell can restore the efficiency, it is presumed that the degradation occurs at that interface. Using this method, researchers have shown that in some BHJ solar cells, the first step of thermal degradation takes place at the interface between the absorber layer and the evaporated metal.[138,139] It is proposed that at elevated temperatures, a polymer-rich layer up to 10 nm thick forms at the interface. In standard architecture devices, electrons are collected at the evaporated metal, and the polymer-rich layer acts as an electron-blocking layer, reducing the solar cell's fill factor and V_{OC}.[138,139]

Rearrangement of the polymer and fullerene in the bulk of the absorber layer is also observed to decrease performance. High efficiency BHJs typically have three phases present – an aggregated polymer phase, an aggregated fullerene phase, and an amorphous phase in which the polymer and fullerene are intimately mixed.[147] Ideally, the aggregated phases are 10–20 nm in size and the fullerene content of the mixed phase is high enough to allow a percolating pathway for electrons (about 20%). When BHJs are heated above T_g for a long enough time, macroscopic phase separation is observed with fullerene aggregates up to several micrometers in size forming.[130,131,148,149] Large scale phase separation decreases a film's ability to separate excitons into free electrons and holes, which takes place at the BHJ interface, so this mechanism usually causes a significant loss of J_{SC}.

In addition to rearrangement of the polymer and fullerene, some research suggests that metal atoms from the electrode can diffuse into the bulk of an organic electronic device and cause degradation.[150–154] Both indium and aluminum atoms have been observed to diffuse into the absorber layer and are thought to act as exciton quenching sites.

5.2. Improving Dark Stability

Several methods of improving the dark stability have been attempted.[155,156] Interfacial degradation via formation of a polymer-rich region is reduced in the inverted architecture. In the inverted architecture, the metal electrode collects holes, and the polymer-rich layer that forms actually improves the performance of those solar cells.[138] Preventing phase separation is accomplished through cross-linking the polymer,[156–159] cross-linking the fullerene,[160–162] or creating a copolymer of polymer and fullerene.[163] Unfortunately, the use of cross-linkable polymers usually results in a lower initial performance compared to the non-cross-linked analogs. Cross-linking the fullerenes also reduces the J_{SC}, which is discussed in the section on photo-induced burn-in. It appears that the best way to avoid thermal degradation is to use materials with a high T_g, as systems with high T_g materials like PCDTBT do not suffer from degradation in the dark at temperatures relevant to solar cell operation.[138,164]

5.3. Photo-Induced Burn-In

Even when they are encapsulated and stable in the dark, many OPVs are observed to degrade rapidly for the first several hundred hours of illumination.[35,37,164] Interestingly, the degradation rate decreases with time and the solar cells can become relatively stable for many thousands of hours afterward. This initial period of fast degradation is called "burn-in."[165] The magnitude of the initial loss can be severe – as shown in Figure 6, a burn-in loss of up to 40% is observed in PCDTBT solar cells,[35–37,166] and PBDTTT-EFT solar cells can burn-in up to 60%.[38] For PCDTBT, the burn-in loss is attributed to an interaction with photons, as no degradation is observed in the dark, even when a current equivalent to short circuit conditions runs through a device (**Figure 8**).[164] A similar photo-induced burn-in is observed in encapsulated BHJs made from regiorandom and regioregular P3HT,[39,167] KP115,[168] quinoxaline based copolymers,[169] and evaporated small molecule OPVs.[170] Researchers have identified a few distinct mechanisms of photo-induced burn-in. In the following sections, we discuss both the device physics that cause the photo-induced reduction of J_{SC} and V_{OC}, as well as their underlying chemical mechanisms. Photo-induced dimerization of fullerenes that decreases exciton-harvesting efficiency is understood to cause J_{SC} loss. An increase in energetic disorder on the polymer in polymer:fullerene BHJs is understood to cause a loss of V_{OC}, though the precise photo-chemical origin remains unclear.

5.3.1. Photo-Induced Jsc Loss by Fullerene Dimerization

A photo-induced loss of J_{SC} is observed in many polymer:PCBM BHJ solar cells (**Figure 9**),[171,172] as well as in evaporated small molecule OPVs that use C60.[170,173,174]

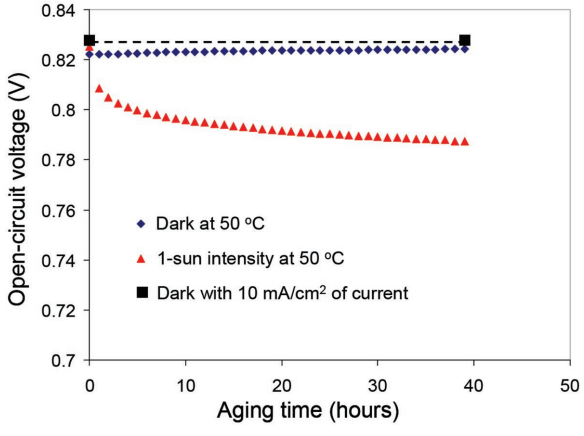

Figure 8. Burn-in in PCDTBT:$PC_{71}BM$ solar cells is not caused by heat or polarons, as heating a cell at 50 °C or driving a current similar to the J_{SC} in the dark does not reproduce the degradation under operation. Only illumination causes the voltage loss. Reproduced with permission.[164] Copyright 2012, Wiley.

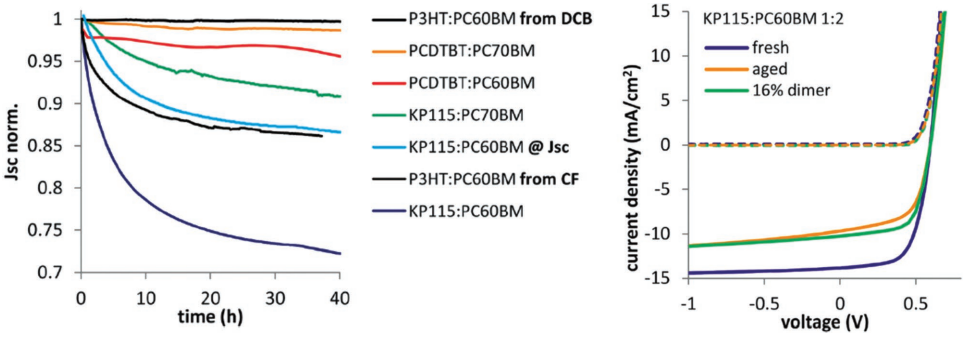

Figure 9. Left) Photo-induced loss of J_{SC} is observed in a variety of polymer:fullerene BHJ OPVs. The extent of J_{SC} loss observed varies among materials systems and processing conditions, and is associated with the extent of fullerene dimerization that occurs. Right) The J–V curves of a fresh and aged solar cell are compared to a fresh solar cell with PCBM dimer intentionally added. The J–V curve for the fresh solar cell with intentionally added dimers that correspond to 16% of total fullerene content lies almost completely on the degraded curve. Reproduced with permission.[172] Copyright 2015, Royal Society of Chemistry.

Loss of external quantum efficiency (EQE) primarily occurs in the absorption region of the fullerene, which implicates their involvement in degradation.[170,172,174] Furthermore, C60 fullerenes are well known to form oligomers upon irradiation, particularly in the absence of oxygen,[175–178] which causes a change in electronic properties.[179] PCBM is known to form dimers under similar conditions.[160,162,180] PCBM dimers in aged BHJ solar cells have been indirectly identified by an increase in the absorption spectra at 320 nm[171,174] and more directly observed through high-performance liquid chromatography (HPLC).[171,172] The reduced J_{SC} observed in degraded solar cells can be reproduced in un-aged solar cells by isolating PCBM dimers using HPLC and intentionally blending them with regular fullerenes. By doing so, researchers can accurately reproduce the J–V curves of degraded BHJ solar cells, which definitively implicates the dimers as the source of current loss (Figure 8, right).[172]

The mechanism by which dimers reduce the J_{SC} is thought to be due to exciton trapping in the fullerene phase, such that excitons formed in the fullerene phase are not efficiently split and collected. Evidence for this mechanism is drawn from the EQE of fresh and aged solar cells.[170,172] In bilayer OPVs, degraded solar cells lose EQE almost entirely in the fullerene absorption wavelengths. A device model that accounts for reduced fullerene exciton diffusion length in aged bilayer films can reproduce the J–V curves of degraded devices very well.[170] This effect is less pronounced in BHJ solar cells, and a reduced exciton diffusion length in the fullerene domain cannot account for the entirety of J_{SC} loss. In these devices, it is proposed that dimerization also affects exciton splitting at polymer-fullerene interfaces, accounting for the reduction of quantum efficiency observed in the polymer absorption region of EQE.[172]

As seen in Figure 8, the relative amount of J_{SC} loss varies among polymer systems and film processing conditions, which suggests that film morphology impacts the amount of dimerization that occurs. Indeed, both the extent of polymer-fullerene mixing and the ordering of the film affect the dimerization reaction. In BHJs made from relatively amorphous polymers like PCDTBT and Si-PCPDTBT where the polymer and fullerene are intimately mixed, dimerization is suppressed. The extent of dimerization and J_{SC} loss is also affected by the voltage condition during aging (Figure 8), and aging the solar cells at V_{OC} condition increases the degradation. Based on these observations, it is suggested that the mechanism of the dimerization reaction occurs via triplet excitons on the fullerene, which would be present in higher concentration at V_{OC} conditions and are more efficiently quenched in highly mixed systems.[172] However, the exact mechanism of dimerization in BHJ films it is not known with certainty.

5.3.2. Photo-Induced V_{OC} Loss and Possible Mechanisms

While light-induced V_{OC} loss occurs in a variety of BHJ solar cells, this particular degradation is most extensively studied in PCDTBT:PC_{71}BM BHJs. As shown in Figure 7, the V_{OC} loss observed in PCDTBT:PC_{71}BM solar cells is directly attributed to an interaction with light. Because the reduced V_{OC} persists even when the metal electrode is peeled off with scotch tape and replaced,[39] when various buffer layers are changed,[35,164] and in both device polarities,[36] the voltage loss is attributed to a bulk process. Defect states that form within the bandgap of aged films and solar cells are directly observed with sensitive absorption techniques, which further confirms this assertion.[164,181–183] The voltage loss during burn-in is shown to correlate well with an increase in energetic disorder on the polymer, which is observed in hole-only diodes of PCDTBT:PC_{71}BM that are illuminated over time (**Figure 10**, left).[164,184] In summary, light-induced defects on PCDTBT are implicated in the photo-induced voltage burn-in.

In general, defect states in BHJ solar cells can reduce the open circuit voltage by one of two mechanisms. Under the first mechanism, the defect states increase the recombination rate constant, reduce the carrier lifetime, and thus reduce the charge carrier density at steady-state.[185,186] This effectively reduces the quasi-fermi level splitting and hence, open circuit voltage. In the second mechanism, the defect states increase the density of states (DOS) near the quasi-fermi level with little to no effect on the recombination rate constant. Though the total charge carrier density at open circuit is not changed, a larger number

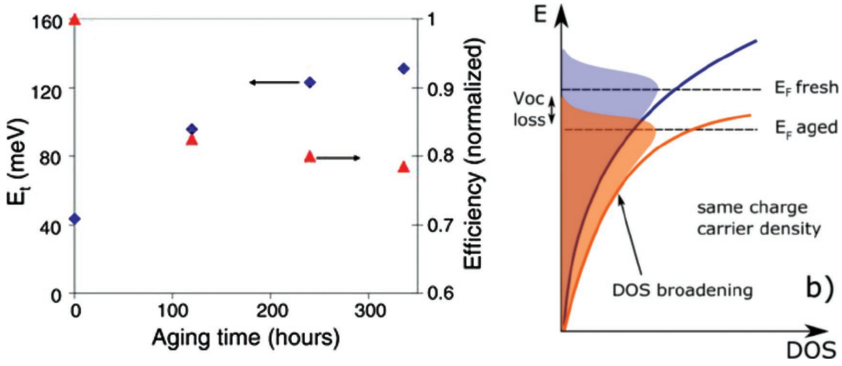

Figure 10. Left) The voltage loss is shown to correlate well with an increase in energetic disorder on the polymer. Reproduced with permission.[164] Copyright 2012, Wiley. Right) A schematic describing the mechanism of VOC loss in polymer:fullerene BHJs. Reproduced with permission.[189] Copyright 2015, Wiley.

of states are available and the charges fill the DOS to a lower energy (Figure 10, right).[187,188] Through a combination of photovoltage decay and charge extraction measurements, it is shown that the charge carrier lifetime and density is the same in aged solar cells as in fresh ones. Instead, the defect states are shown to cause an increase in the DOS, which is understood to cause the voltage loss.[189]

Several hypotheses attempt to account for the chemical origin of the defect states that cause DOS broadening. Because the burn-in degradation slows down and eventually stops, some have suggested that there are a limited number of reactive species or reaction sites that are consumed during burn-in. Polymer chain ends, which still contain the monomer's reactive capping groups, or impurities such as bromine and palladium left over from synthesis are some suggested reactive species.[164,190,191] Indeed, PCDTBT solar cells with a higher concentration of palladium burn-in to a greater extent than purer batches, and bromine at chain ends also empirically affect burn-in.[190,191] Another model suggests that a C—H bond is broken on a polymer side chain and the hydrogen abstracts onto the conjugated core, creating electronic defect states. While breaking of a C—H bond requires energies upwards of 4 eV, their modeling suggests a defect pair may form with as little energy as 2.2 eV. Over time, a steady-state concentration of these defect pairs could build up in the solar cell, allowing burn-in to eventually end.[182] Photo-induced crosslinking among polymer chains and between polymer chains and fullerene molecules is also discussed in the literature. In this model, burn-in is thought to end when the motion of the polymer is hindered by the cross-linking, such that the spatial rearrangement necessary for further chemical reaction is prevented.[192] Cross-linking also accounts for the self-limiting nature of the kinetics. The formation of long-lived free-radical species in polymer films is also suggested as the source of voltage loss. One study indicates a negative correlation between the concentration of free-radical species in commercially purchased polymers and initial BHJ V_{OC}.[193] Electron spin resonance measurements of neat OPV polymer films illuminated under inert conditions shows an increase in free-radical concentration over illumination time (**Figure 11**).[88] More research is needed in this area.

5.4. Decreasing Photo-Induced Burn-In

Removing halide and metal impurities, increasing material crystallinity, and reducing initial energetic disorder are all routes to improving the photo-stability of encapsulated OPVs. It is well known that the presence of halide and metals from synthesis can lower the initial performance of OPVs,[190,194–197] and it was recently shown that the concentration of each can affect the magnitude of photo-induced burn-in.[190,191] Keeping the concentrations of these impurities low should help reduce burn-in loss for all OPVs. Making OPVs with more ordered film morphologies also reduces burn-in. The photo-dimerization reaction that causes J_{SC} loss is suppressed in PCBM films that are annealed into a crystalline morphology.[172] Dimerization can be further eliminated by using C70, $PC_{71}BM$, or higher adduct fullerenes that do not appear to form dimers.[171] In polymer BHJs, solar cells made with crystalline polymers like regioregular P3HT and KP115 lose less efficiency than more amorphous ones like PCDTBT and regiorandom P3HT.[39] Two effects could lead to the improved stability of more ordered film morphologies. As previously discussed, more ordered film morphologies are generally more stable to chemical change. Ordered film morphologies may also be more tolerant to defect states introduced during degradation, as they begin with less energetic disorder than amorphous films.[189] When PCDTBT is carefully fractionated to separate and remove lower molecular weight portions of the molecular weight distribution, the initial energetic disorder of BHJ films is reduced. This procedure not only improves the initial performance of the solar cells, but also reduces the photo-induced increase in energetic disorder and improves the stability to photo-induced burn-in.[184]

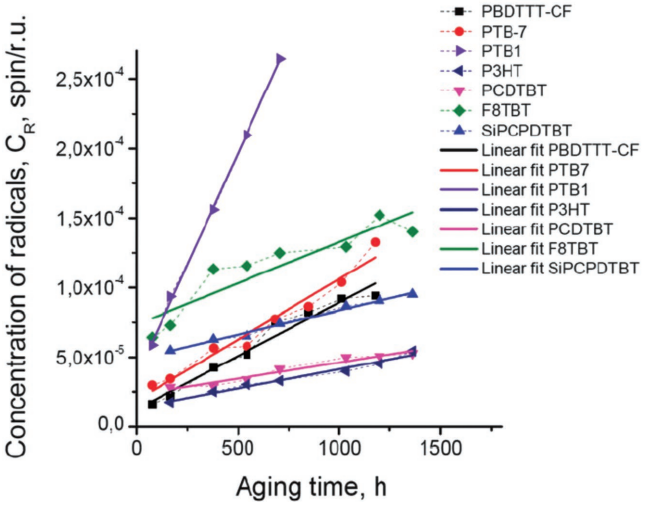

Figure 11. Free-radicals can be detected in polymer films using ESR. The concentration of free-radicals increases in each polymer with aging time under inert conditions. Both the initial concentration and rate of increase vary for different polymers. Reproduced with permission.[88] Copyright 2015, Royal Society of Chemistry.

To date, no solution-processed materials are free of photo-induced burn-in. However, significantly reduced burn-in is reported for some evaporated small-molecule solar cells.[198,199] Intrinsic degradation of OLED devices has been significantly reduced, and materials are sufficiently stable to be in commercial products.[200] It is worth noting that the commercially viable OLEDs are also evaporated small-molecules, mostly because of improved stability. Organic pigments, which are chemically similar to OLED and OPV materials but are also insoluble, can maintain color for years even with direct exposure to oxygen and water.[95] They are used in a variety of car paints. As it stands today, the path to eliminating photo-induced burn-in may point to only using evaporated or insoluble molecules.

6. Conclusions, Recommendations and Outlook

Even with uncertainty regarding the mechanisms of photo-induced burn-in, some general recommendations for improving the stability of OPVs can be made. First, OPVs must be encapsulated to achieve long-term stability. Even though the stability of the OPV materials can be improved with ordered and dense film morphologies or elimination of side chains, the long-term rate of oxidation of electrode materials and absorber layers is limited by the diffusion rate of oxygen and water into the devices. Glass-on-glass encapsulation or flexible barrier materials are necessary to sufficiently slow oxygen and water permeation for OPV lifetimes greater than 10 years. Research effort into reducing the cost and improving the performance of flexible barrier films is necessary to improve the commercial viability of OPVs. Second, the OPV materials themselves must have high glass transition temperatures relative to the operating conditions to achieve stability in the dark. T_g's greater than 100 °C should be sufficient and are desired. Low molecular weight species, which can diffuse readily and act as plasticizing agents to reduce the T_g, should likely be avoided.

The area most in need of further research is photo-induced burn-in, as 10–50% relative efficiency is lost even in well-encapsulated devices. To put into proper perspective, burn-in loss is essentially a down grade of 10–50% in initial efficiency. For a technology that already has relatively low starting efficiency, burn-in loss is particularly harmful. Furthermore, the cause of photo-induced V_{OC} is not as well understood as the other degradation mechanisms. The kinetics of burn-in are particularly interesting – it is not presently clear why burn-in lasts for several hundred hours and then apparently stops. A more complete understanding of the photo-induced V_{OC} loss is still necessary, as most recommendations to improve voltage stability are more empirical in nature. For instance, while photo-stability of the materials is improved when halide and metal impurities are kept sufficiently low and the photo-induced increase in energetic disorder can be suppressed in more ordered materials, the precise chemical origin behind these guidelines is still in contention.

In order to facilitate future research, we recommend a more rapid experimental iteration will be helpful to both identify promising materials and improve mechanistic understanding. Stability screening must include illumination. Unlike crystalline silicon, these solar cells significantly degrade under light, so screening tests like the 85/85 test that tests a solar cell or module's stability to 85 °C and 85% relative humidity, are not sufficient. Quick and simple screening experiments can be used to "pass or fail" new materials. For example, if solar cells are not stable at slightly elevated temperatures of 80–100 °C, then they "fail" at intrinsic dark stability and therefore do not present a promising material combination or architecture. Illumination testing does not need to last long – fortunately, photo-induced burn-in usually ends after several hundred hours. Future researchers can further speed testing with LED arrays that can provide light intensity beyond 1 sun. While degradation may not scale perfectly linearly with intensity, concentrated light could dramatically accelerate research on burn-in.

While further research is necessary, there are some promising points in the outlook of OPV. First, OPV solar cells with extrapolated lifetimes greater than 20 years have been observed. Before this observation, it was not necessarily assumed that an organic material could withstand repeated photo-excitation for so long. If encapsulation is good enough, at least some OPV materials can be long-term stable. Second, some forms of degradation are now well understood and preventable. Using materials with a high glass transition temperature can easily prevent intrinsic degradation in the dark. Fullerene dimerization can be avoided by using C70, $PC_{71}BM$, or higher adduct fullerenes that do not form dimers. If C60 or PCBM must be used, dimerization can be suppressed in ordered fullerene phases. Third, there are promising clues to reducing V_{OC} and FF burn-in. Evaporated OLEDs are commercially viable, and evaporated small-molecule OPVs are also promising. Organic pigments, which are dense, insoluble molecules, can show remarkable stability even in ambient. The field should further explore OPVs made from similar materials with high density and low solubility. With such changes to material design, it may be possible for OPVs to achieve stable long-term performance.

Acknowledgements

The authors would like to thank Craig Peters, Toby Sachs-Quintana, Thomas Heumueller, Rongrong Cheacharoen, Christopher Bruner, Stephanie Dupont, and Professor Reinhold Dauskardt for insight and discussion on this topic over the years. The authors also acknowledge funding from the Office of Naval Research Award No. N00014-14-1-0580 and N00014-14-1-0280 and the King Abdullah University of Science and Technology.

Received: July 25, 2016
Revised: September 12, 2016
Published online:

[1] D. M. DeLongchamp, in *Semicond. Mater. Sol. Photovolt. Cells* (Eds.: S. Das, K. C. Mandal, R. N. Bhattacharya), Springer, **2016**, pp. 25–74.
[2] C. J. Mulligan, C. Bilen, X. Zhou, W. J. Belcher, P. C. Dastoor, *Sol. Energy Mater. Sol. Cells* **2015**, *133*, 26.
[3] S. B. Darling, F. You, *RSC Adv.* **2013**, *3*, 17633.
[4] C. J. Mulligan, M. Wilson, G. Bryant, B. Vaughan, X. Zhou, W. J. Belcher, P. C. Dastoor, *Sol. Energy Mater. Sol. Cells* **2014**, *120*, 9.

[5] N. Espinosa, R. García-Valverde, A. Urbina, F. Lenzmann, M. Manceau, D. Angmo, F. C. Krebs, *Sol. Energy Mater. Sol. Cells* **2012**, *97*, 3.
[6] M. Jørgensen, J. E. Carlé, R. R. Søndergaard, M. Lauritzen, N. A. Dagnæs-Hansen, S. L. Byskov, T. R. Andersen, T. T. Larsen-Olsen, A. P. L. Böttiger, B. Andreasen, L. Fu, L. Zuo, Y. Liu, E. Bundgaard, X. Zhan, H. Chen, F. C. Krebs, *Sol. Energy Mater. Sol. Cells* **2013**, *119*, 84.
[7] F. C. S. P. Thanks, M. Pfeiffer, "*Heliatek sets new Organic Photovoltaic world record efficiency of 13.2%,*" http://www.heliatek.com/en/press/press-releases/details/heliatek-sets-new-organic-photovoltaic-world-record-efficiency-of-13-2 **2016** (accessed: Nov 2016).
[8] Y. Liu, J. Zhao, Z. Li, C. Mu, W. Ma, H. Hu, K. Jiang, H. Lin, H. Ade, H. Yan, *Nat. Commun.* **2014**, *5*, 5293.
[9] M. A. Green, K. Emery, Y. Hishikawa, W. Warta, E. D. Dunlop, *Prog. Photovoltaics Res. Appl.* **2016**, *24*, 3.
[10] H. Zhou, Y. Zhang, C.-K. Mai, S. D. Collins, G. C. Bazan, T.-Q. Nguyen, A. J. Heeger, *Adv. Mater.* **2015**, *27*, 1676.
[11] J. You, L. Dou, K. Yoshimura, T. Kato, K. Ohya, T. Moriarty, K. Emery, C.-C. Chen, J. Gao, G. Li, Y. Yang, *Nat. Commun.* **2013**, *4*, 1.
[12] Heliatek, *Heliatek Sets New World Record Efficiency of 10.7% for Its Organic Tandem Cell,* http://www.heliatek.com/en/press/press-releases/details/heliatek-sets-new-world-record-efficiency-of-107-for-its-organic-tandem-cell **2012**, (accessed: Nov 2016).
[13] T. Liu, L. Huo, X. Sun, B. Fan, Y. Cai, T. Kim, J. Y. Kim, H. Choi, Y. Sun, *Adv. Energy Mater.* **2015**, 1502109.
[14] R. A. J. Janssen, J. Nelson, *Adv. Mater.* **2013**, *25*, 1847.
[15] *Facts about Solar Technology from SunPower* http://us.sunpower.com/solar-panels-technology/facts/, **2014** (accessed: Nov 2016).
[16] B. Azzopardi, C. J. M. Emmott, A. Urbina, F. C. Krebs, J. Mutale, J. Nelson, *Energy Environ. Sci.* **2011**, *4*, 3741.
[17] J. Y. Jeng, Y. F. Chiang, M. H. Lee, S. R. Peng, T. F. Guo, P. Chen, T. C. Wen, *Adv. Mater.* **2013**, *25*, 3727.
[18] O. Malinkiewicz, A. Yella, Y. H. Lee, G. M. M. Espallargas, M. Graetzel, M. K. Nazeeruddin, H. J. Bolink, *Nat. Photonics* **2014**, *8*, 128.
[19] S. N. Habisreutinger, T. Leijtens, G. E. Eperon, S. D. Stranks, R. J. Nicholas, H. J. Snaith, **2014**.
[20] G. Yu, J. Gao, J. C. Hummelen, F. Wudl, A. J. Heeger, *Science* **1995**, *270*, 1789.
[21] C.-Z. Li, H.-L. Yip, A. K.-Y. Jen, *J. Mater. Chem.* **2012**, *22*, 4161.
[22] P. M. Beaujuge, J. M. J. Fréchet, *J. Am. Chem. Soc.* **2011**, *133*, 20009.
[23] P.-L. T. Boudreault, A. Najari, M. Leclerc, *Chem. Mater.* **2011**, *23*, 456.
[24] Z. Zhang, J. Wang, *J. Mater. Chem.* **2012**, *22*, 4178.
[25] A. W. Hains, Z. Liang, M. A. Woodhouse, B. A. Gregg, *Chem. Rev.* **2010**, *110*, 6689.
[26] E. L. Ratcliff, B. Zacher, N. R. Armstrong, *J. Phys. Chem. Lett.* **2011**, *2*, 1337.
[27] L. Lu, T. Zheng, Q. Wu, A. M. Schneider, D. Zhao, L. Yu, *Chem. Rev.* **2015**, *115*, 12666.
[28] J. Hou, X. Guo, in *Org. Sol. Cells* (Ed.: W. C. H. Choy), Springer London, London, **2013**.
[29] G. Li, R. Zhu, Y. Yang, *Nat. Photonics* **2012**, *6*, 153.
[30] E. A. Katz, S. Gevorgyan, M. S. Orynbayev, F. C. Krebs, *Eur. Phys. J. Appl. Phys.* **2007**, *36*, 307.
[31] M. Corazza, F. C. Krebs, S. A. Gevorgyan, *Sol. Energy Mater. Sol. Cells* **2015**, *143*, 467.
[32] Y. Zhang, E. Bovill, J. Kingsley, A. R. Buckley, H. Yi, A. Iraqi, T. Wang, D. G. Lidzey, *Sci. Rep.* **2016**, *6*, 21632.
[33] E. Voroshazi, B. Verreet, T. Aernouts, P. Heremans, *Sol. Energy Mater. Sol. Cells* **2011**, *95*, 1303.
[34] H. Hintz, H.-J. Egelhaaf, L. Lüer, J. Hauch, H. Peisert, T. Chassé, *Chem. Mater.* **2011**, *23*, 145.
[35] R. Roesch, K.-R. Eberhardt, S. Engmann, G. Gobsch, H. Hoppe, *Sol. Energy Mater. Sol. Cells* **2013**, *117*, 59.
[36] W. R. Mateker, I. T. Sachs-Quintana, G. F. Burkhard, R. Cheacharoen, M. D. McGehee, *Chem. Mater.* **2015**, *27*, 404.
[37] C. H. Peters, I. T. Sachs-Quintana, J. P. Kastrop, S. Beaupré, M. Leclerc, M. D. McGehee, *Adv. Energy Mater.* **2011**, *1*, 491.
[38] A. J. Pearson, P. E. Hopkinson, E. Couderc, K. Domanski, M. Abdi-Jalebi, N. C. Greenham, *Org. Electron.* **2016**, *30*, 225.
[39] T. Heumueller, W. R. Mateker, I. T. Sachs-Quintana, K. Vandewal, J. A. Bartelt, T. M. Burke, T. Ameri, C. J. Brabec, M. D. McGehee, *Energy Environ. Sci.* **2014**, *7*, 2974.
[40] M. Koehl, M. Heck, S. Wiesmeier, J. Wirth, *Sol. Energy Mater. Sol. Cells* **2011**, *95*, 1638.
[41] J. E. Carlé, M. Helgesen, M. V. Madsen, E. Bundgaard, F. C. Krebs, *J. Mater. Chem. C* **2014**, *2*, 12901297.
[42] M. Hösel, R. R. Søndergaard, M. Jørgensen, F. C. Krebs, *Adv. Eng. Mater.* **2013**, *15*, 1068.
[43] D. M. Tanenbaum, H. F. Dam, R. Rosch, M. Jørgensen, H. Hoppe, F. C. Krebs, *Sol. Energy Mater. Sol. Cells* **2012**, *97*, 157.
[44] R. Tipnis, J. Bernkopf, S. Jia, J. Krieg, S. Li, M. Storch, D. Laird, *Sol. Energy Mater. Sol. Cells* **2009**, *93*, 442.
[45] J. Adams, M. Salvador, L. Lucera, S. Langner, G. D. Spyropoulos, F. W. Fecher, M. M. Voigt, S. A. Dowland, A. Osvet, H.-J. Egelhaaf, C. J. Brabec, *Adv. Energy Mater.* **2015**, *5*, 1501065.
[46] J. Adams, G. D. Spyropoulos, M. Salvador, N. Li, S. Strohm, L. Lucera, S. Langner, F. Machui, H. Zhang, T. Ameri, M. M. Voigt, F. C. Krebs, C. J. Brabec, *Energy Environ. Sci.* **2014**, *00*, 1.
[47] S. A. Gevorgyan, M. Jørgensen, F. C. Krebs, K. O. Sylvester-Hvid, *Sol. Energy Mater. Sol. Cells* **2011**, *95*, 1389.
[48] P. Romero-Gomez, R. Betancur, A. Martinez-Otero, X. Elias, M. Mariano, B. Romero, B. Arredondo, R. Vergaz, J. Martorell, *Sol. Energy Mater. Sol. Cells* **2015**, *137*, 44.
[49] Z. Kam, X. Wang, J. Zhang, J. Wu, *Appl. Mater. Interfaces* **2015**, *7*, 1608.
[50] M. O. Reese, S. A. Gevorgyan, M. Jørgensen, E. Bundgaard, S. R. Kurtz, D. S. Ginley, D. C. Olson, M. T. Lloyd, P. Morvillo, E. A. Katz, A. Elschner, O. Haillant, T. R. Currier, V. Shrotriya, M. Hermenau, M. Riede, K. R. Kirov, G. Trimmel, T. Rath, O. Inganäs, F. Zhang, M. Andersson, K. Tvingstedt, M. Lira-Cantu, D. Laird, C. McGuiness, S. Gowrisanker, M. Pannone, M. Xiao, J. Hauch, R. Steim, D. M. Delongchamp, R. Rösch, H. Hoppe, N. Espinosa, A. Urbina, G. Yaman-Uzunoglu, J. B. Bonekamp, A. J. J. M. Van Breemen, C. Girotto, E. Voroshazi, F. C. Krebs, *Sol. Energy Mater. Sol. Cells* **2011**, *95*, 1253.
[51] F. C. Krebs, S. A. Gevorgyan, B. Gholamkhass, S. Holdcroft, C. Schlenker, M. E. Thompson, B. C. Thompson, D. Olson, D. S. Ginley, S. E. Shaheen, H. N. Alshareef, J. W. Murphy, W. J. Youngblood, N. C. Heston, J. R. Reynolds, S. Jia, D. Laird, S. M. Tuladhar, J. G. A. Dane, P. Atienzar, J. Nelson, J. M. Kroon, M. M. Wienk, R. A. J. Janssen, K. Tvingstedt, F. Zhang, M. Andersson, O. Inganäs, M. Lira-Cantu, R. de Bettignies, S. Guillerez, T. Aernouts, D. Cheyns, L. Lutsen, B. Zimmermann, U. Würfel, M. Niggemann, H.-F. Schleiermacher, P. Liska, M. Grätzel, P. Lianos, E. A. Katz, W. Lohwasser, B. Jannon, *Sol. Energy Mater. Sol. Cells* **2009**, *93*, 1968.
[52] S. A. Gevorgyan, O. Zubillaga, J. M. V. de Seoane, M. Machado, E. A. Parlak, N. Tore, E. Voroshazi, T. Aernouts, H. Müllejans, G. Bardizza, N. Taylor, W. J. H. Verhees, J. M. Kroon, P. Morvillo, C. Minarini, F. Roca, F. a. Castro, S. Cros, B. Lechêne, J. F. Trigo, C. Guillén, J. Herrero, B. Zimmermann, S. B. Sapkota, C. Veit, U. Würfel, P. S. Tuladhar, J. R. Durrant, S. Winter,

S. Rousu, M. Välimäki, V. Hinrichs, S. R. Cowan, D. C. Olson, P. Sommer-Larsen, F. C. Krebs, *Renew. Energy* **2014**, *63*, 376.
[53] R. Rösch, D. M. Tanenbaum, M. Jørgensen, M. Seeland, M. Bärenklau, M. Hermenau, E. Voroshazi, M. T. Lloyd, Y. Galagan, B. Zimmermann, U. Würfel, M. Hösel, H. F. Dam, S. a. Gevorgyan, S. Kudret, W. Maes, L. Lutsen, D. Vanderzande, R. Andriessen, G. Teran-Escobar, M. Lira-Cantu, A. Rivaton, G. Y. Uzunoğlu, D. Germack, B. Andreasen, M. V. Madsen, K. Norrman, H. Hoppe, F. C. Krebs, *Energy Environ. Sci.* **2012**, *5*, 6521.
[54] S. A. Gevorgyan, A. J. Medford, E. Bundgaard, S. B. Sapkota, H. F. Schleiermacher, B. Zimmermann, U. Würfel, A. Chafiq, M. Lira-Cantu, T. Swonke, M. Wagner, C. J. Brabec, O. Haillant, E. Voroshazi, T. Aernouts, R. Steim, J. a. Hauch, A. Elschner, M. Pannone, M. Xiao, A. Langzettel, D. Laird, M. T. Lloyd, T. Rath, E. Maier, G. Trimmel, M. Hermenau, T. Menke, K. Leo, R. Rösch, M. Seeland, H. Hoppe, T. J. Nagle, K. B. Burke, C. J. Fell, D. Vak, T. B. Singh, S. E. Watkins, Y. Galagan, A. Manor, E. a. Katz, T. Kim, K. Kim, P. M. Sommeling, W. J. H. Verhees, S. C. Veenstra, M. Riede, M. Greyson Christoforo, T. Currier, V. Shrotriya, G. Schwartz, F. C. Krebs, *Sol. Energy Mater. Sol. Cells* **2011**, *95*, 1398.
[55] R. Roesch, T. Faber, E. von Hauff, T. M. Brown, M. Lira-Cantu, H. Hoppe, *Adv. Energy Mater.* **2015**, *5*, 1501407.
[56] M. T. Lloyd, C. H. Peters, A. Garcia, I. V. Kauvar, J. J. Berry, M. O. Reese, M. D. McGehee, D. S. Ginley, D. C. Olson, *Sol. Energy Mater. Sol. Cells* **2011**, *95*, 1382.
[57] K. Feron, T. J. Nagle, L. J. Rozanski, B. B. Gong, C. J. Fell, *Sol. Energy Mater. Sol. Cells* **2013**, *109*, 169.
[58] D. Angmo, P. M. Sommeling, R. Gupta, M. Hösel, S. A. Gevorgyan, J. M. Kroon, G. U. Kulkarni, F. C. Krebs, *Adv. Eng. Mater.* **2014**, *16*, 976.
[59] K. Norrman, F. C. Krebs, *Sol. Energy Mater. Sol. Cells* **2006**, *90*, 213.
[60] N. Kim, W. J. Potscavage, A. Sundaramoothi, C. Henderson, B. Kippelen, S. Graham, *Sol. Energy Mater. Sol. Cells* **2012**, *101*, 140.
[61] V. D. Mihailetchi, P. W. M. Blom, J. C. Hummelen, M. T. Rispens, *J. Appl. Phys.* **2003**, *94*, 6849.
[62] C. J. Brabec, A. Cravino, D. Meissner, N. S. Sariciftci, T. Fromherz, M. T. Rispens, L. Sanchez, J. C. Hummelen, *Adv. Funct. Mater.* **2001**, *11*, 374.
[63] S. Cros, M. Firon, S. Lenfant, P. Trouslard, L. Beck, *Nucl. Instruments Methods Phys. Res. Sect. B* **2006**, *251*, 257.
[64] P. E. Burrows, V. Bulovic, S. R. Forrest, L. S. Sapochak, D. M. McCarty, M. E. Thompson, *Appl. Phys. Lett.* **1994**, *65*, 2922.
[65] J. Buseman-Williams, K. D. Frischknecht, M. D. Hubert, A. K. Saafir, J. D. Tremel, *J. Soc. Inf. Disp.* **2007**, *15*, 103.
[66] F. So, D. Kondakov, *Adv. Mater.* **2010**, *22*, 3762.
[67] E. Voroshazi, B. Verreet, A. Buri, R. Müller, D. Di Nuzzo, P. Heremans, *Org. Electron.* **2011**, *12*, 736.
[68] C. E. Small, S. Chen, J. Subbiah, C. M. Amb, S. Tsang, T. Lai, J. R. Reynolds, F. So, *Nat. Photonics* **2011**, *6*, 115.
[69] M. T. Lloyd, D. C. Olson, P. Lu, E. Fang, D. L. Moore, M. S. White, M. O. Reese, D. S. Ginley, J. W. P. Hsu, *J. Mater. Chem.* **2009**, *19*, 7638.
[70] S. K. Hau, H.-L. Yip, N. S. Baek, J. Zou, K. O'Malley, A. K.-Y. Jen, *Appl. Phys. Lett.* **2008**, *92*, 253301.
[71] A. Rivaton, J.-L. Gardette, B. Mailhot, S. Morlat-Therlas, *Macromol. Symp.* **2005**, *225*, 129.
[72] A. Rivaton, A. Tournebize, J. Gaume, P.-O. Bussière, J.-L. Gardette, S. Therias, *Polym. Int.* **2014**, *63*, 1335.
[73] M. O. Reese, A. M. Nardes, B. L. Rupert, R. E. Larsen, D. C. Olson, M. T. Lloyd, S. E. Shaheen, D. S. Ginley, G. Rumbles, N. Kopidakis, *Adv. Funct. Mater.* **2010**, *20*, 3476.
[74] A. Tournebize, A. Rivaton, J. L. Gardette, C. Lombard, B. Pépin-Donat, S. Beaupré, M. Leclerc, *Adv. Energy Mater.* **2014**, *4*, 1.
[75] S. Chambon, A. Rivaton, J. Gardette, M. Firon, L. Lutsen, *J. Polym. Sci. A Polym. Chem.* **2006**, *45*, 317.
[76] S. Chambon, A. Rivaton, J. Gardette, M. Firon, *J. Polym. Sci. A Polym. Chem.* **2009**, *47*, 6044.
[77] M. Manceau, A. Rivaton, J.-L. Gardette, S. Guillerez, N. Lemaître, *Polym. Degrad. Stab.* **2009**, *94*, 898.
[78] N. Sai, K. Leung, J. Zádor, G. Henkelman, *Phys. Chem. Chem. Phys.* **2014**, *16*, 8092.
[79] A. Dupuis, P. Wong-Wah-Chung, A. Rivaton, J.-L. Gardette, *Polym. Degrad. Stab.* **2012**, *97*, 366.
[80] M. Manceau, A. Rivaton, J.-L. Gardette, *Macromol. Rapid Commun.* **2008**, *29*, 1823.
[81] P.-O. Bussière, A. Rivaton, S. Thérias, J.-L. Gardette, *J. Phys. Chem. B* **2012**, *116*, 802.
[82] A. Tournebize, P.-O. Bussière, P. Wong-Wah-Chung, S. Thérias, A. Rivaton, J.-L. Gardette, S. Beaupré, M. Leclerc, *Adv. Energy Mater.* **2013**, *3*, 478.
[83] J. Razzell-Hollis, J. Wade, W. C. Tsoi, Y. Soon, J. Durrant, J.-S. Kim, *J. Mater. Chem. A* **2014**, *2*, 20189.
[84] S. Shah, R. Biswas, *J. Phys. Chem. C* **2015**, *119*, 20265.
[85] A. Tournebize, J.-L. Gardette, C. Taviot-Guého, D. Bégué, M. A. Arnaud, C. Dagron-Lartigau, H. Medlej, R. C. Hiorns, S. Beaupré, M. Leclerc, A. Rivaton, *Polym. Degrad. Stab.* **2015**, *112*, 175.
[86] I. Fraga Domínguez, P. D. Topham, P.-O. Bussière, D. Bégué, A. Rivaton, *J. Phys. Chem. C* **2015**, *119*, 2166.
[87] P. Henriksson, C. Lindqvist, B. Abdisa, E. Wang, Z. George, R. Kroon, C. Müller, T. Yohannes, O. Inganäs, M. R. Andersson, *Sol. Energy Mater. Sol. Cells* **2014**, *130*, 138.
[88] L. A. Frolova, N. P. Piven, D. K. Susarova, A. V. Akkuratov, S. D. Babenko, P. A. Troshin, *Chem. Commun.* **2015**, *51*, 2242.
[89] M. Manceau, M. Helgesen, F. C. Krebs, *Polym. Degrad. Stab.* **2010**, *95*, 2666.
[90] M. Manceau, E. Bundgaard, J. E. Carlé, O. Hagemann, M. Helgesen, R. Søndergaard, M. Jørgensen, F. C. Krebs, *J. Mater. Chem.* **2011**, *21*, 4132.
[91] Y. W. Soon, S. Shoaee, R. S. Ashraf, H. Bronstein, B. C. Schroeder, W. Zhang, Z. Fei, M. Heeney, I. McCulloch, J. R. Durrant, *Adv. Funct. Mater.* **2014**, *24*, 1474.
[92] W. R. Mateker, T. Heumueller, R. Cheacharoen, I. T. Sachs-Quintana, J. Warnan, X. Liu, G. C. Bazan, P. M. Beaujuge, M. D. McGehee, *Chem. Mater.* **2015**, *27*, 6345.
[93] V. Ramamurthy, K. Venkatesan, *Chem. Rev.* **1987**, *87*, 433.
[94] A. Whitaker, *J. Soc. Dye. Color.* **1978**, *94*, 431.
[95] P. Erk, in *High Perform. Pigment.* (Ed.: H. M. Smith), Wiley-VCH Verlag GmbH & Co. KGaA, **2002**, pp. 103–123.
[96] S. Qu, H. Tian, *Chem. Commun.* **2012**, *48*, 3039.
[97] M. U. Schmidt, D. W. M. Hofmann, C. Buchsbaum, H. J. Metz, *Angew. Chemie* **2006**, *45*, 1313.
[98] S. Chambon, A. Rivaton, J.-L. Gardette, M. Firon, *Sol. Energy Mater. Sol. Cells* **2007**, *91*, 394.
[99] M. Manceau, A. Rivaton, J. L. Gardette, S. Guillerez, N. Lemaître, *Sol. Energy Mater. Sol. Cells* **2011**, *95*, 1315.
[100] E. T. Hoke, I. T. Sachs-Quintana, M. T. Lloyd, I. Kauvar, W. R. Mateker, A. M. Nardes, C. H. Peters, N. Kopidakis, M. D. McGehee, *Adv. Energy Mater.* **2012**, *2*, 1351.
[101] A. J. Heeger, *Adv. Mater.* **2014**, *26*, 10.
[102] I. C. Wang, L. A. Tai, D. D. Lee, P. P. Kanakamma, C. K. F. Shen, T. Y. Luh, C. H. Cheng, K. C. Hwang, *J. Med. Chem.* **1999**, *42*, 4614.
[103] H. Neugebauer, C. Brabec, J. C. Hummelen, N. S. Sariciftci, *Sol. Energy Mater. Sol. Cells* **2000**, *61*, 35.

[104] S. Heutz, P. Sullivan, B. Sanderson, S. Schultes, T. Jones, *Sol. Energy Mater. Sol. Cells* **2004**, *83*, 229.
[105] K. Kawano, R. Pacios, D. Poplavskyy, J. Nelson, D. D. C. Bradley, J. R. Durrant, *Sol. Energy Mater. Sol. Cells* **2006**, *90*, 3520.
[106] J. M. Kroon, M. M. Wienk, W. J. H. Verhees, J. C. Hummelen, *Thin Solid Films* **2002**, *403–404*, 223.
[107] G. Dennler, C. Lungenschmied, H. Neugebauer, N. S. Sariciftci, M. Latrèche, G. Czeremuszkin, M. R. Wertheimer, *Thin Solid Films* **2006**, *511–512*, 349.
[108] N. Kim, S. Graham, *Thin Solid Films* **2013**, *547*, 57.
[109] S. B. Sapkota, A. Spies, B. Zimmermann, I. Dürr, U. Würfel, *Sol. Energy Mater. Sol. Cells* **2014**, *130*, 144.
[110] G. L. Graff, R. E. Williford, P. E. Burrows, *J. Appl. Phys.* **2004**, *96*, 1840.
[111] A. G. Erlat, B. M. Henry, C. R. M. Grovenor, A. G. D. Briggs, R. J. Chater, Y. Tsukahara, *J. Phys. Chem. B* **2004**, *108*, 883.
[112] M. P. Nikiforov, J. Strzalka, S. B. Darling, *Sol. Energy Mater. Sol. Cells* **2013**, *110*, 36.
[113] P. E. Burrows, G. L. Graff, M. E. Gross, P. M. Martin, M. Hall, E. Mast, C. Bonham, W. Bennet, L. Michalski, M. Weaver, J. J. Brown, D. Fogarty, L. S. Sapochak, *Proc. SPIE* **2001**, *4105*, 75.
[114] M. D. Groner, S. M. George, R. S. McLean, P. F. Carcia, *Appl. Phys. Lett.* **2006**, *88*, 051907.
[115] J. Ahmad, K. Bazaka, L. J. Anderson, R. D. White, M. V. Jacob, *Renew. Sustain. Energy Rev.* **2013**, *27*, 104.
[116] D. Yu, Y.-Q. Yang, Z. Chen, Y. Tao, Y.-F. Liu, *Opt. Commun.* **2015**, 1.
[117] Vitriflex, "Flexible Ulra-Barriers," http://www.vitriflex.com/technology/ (accessed: Sept 2016).
[118] S. Savagatrup, A. D. Printz, T. F. O'Connor, A. V. Zaretski, D. Rodriquez, E. J. Sawyer, K. M. Rajan, R. I. Acosta, S. E. Root, D. J. Lipomi, *Energy Environ. Sci.* **2014**, *8*, 55.
[119] O. K. Oyewole, D. Yu, J. Du, J. Asare, V. C. Anye, A. Fashina, M. G. Zebaze Kana, W. O. Soboyejo, *J. Appl. Phys.* **2015**, *118*, 075302.
[120] F. C. Krebs, H. Spanggard, T. Kjaer, M. Biancardo, J. Alstrup, *Mater. Sci. Eng. B* **2007**, *138*, 106.
[121] V. Balcaen, N. Rolston, S. R. Dupont, E. Voroshazi, R. H. Dauskardt, *Sol. Energy Mater. Sol. Cells* **2015**, *143*, 418.
[122] S. R. Dupont, E. Voroshazi, P. Heremans, R. H. Dauskardt, *Org. Electron. Phys. Mater. Appl.* **2013**, *14*, 1262.
[123] V. Brand, C. Bruner, R. H. Dauskardt, *Sol. Energy Mater. Sol. Cells* **2012**, *99*, 182.
[124] S. R. Dupont, M. Oliver, F. C. Krebs, R. H. Dauskardt, *Sol. Energy Mater. Sol. Cells* **2012**, *97*, 171.
[125] S. R. Dupont, E. Voroshazi, D. Nordlund, R. H. Dauskardt, *Sol. Energy Mater. Sol. Cells* **2014**, *132*, 443.
[126] S. Savagatrup, D. Rodriquez, A. D. Printz, A. B. Sieval, J. C. Hummelen, D. J. Lipomi, *Chem. Mater.* **2015**, *27*, 3902.
[127] N. R. Tummala, C. Bruner, C. Risko, J. L. Brédas, R. H. Dauskardt, *ACS Appl. Mater. Interfaces* **2015**, *7*, 9957.
[128] C. Bruner, R. Dauskardt, *Macromolecules* **2013**, *47*, 1117.
[129] F. Padinger, T. Fromherz, P. Denk, C. J. Brabec, J. Zettner, T. Hierl, N. S. Sariciftci, *Synth. Met.* **2001**, *121*, 1605.
[130] X. Yang, J. K. J. van Duren, R. A. J. Janssen, M. A. J. Michels, J. Loos, *Macromolecules* **2004**, *37*, 2151.
[131] S. Bertho, I. Haeldermans, A. Swinnen, W. Moons, T. Martens, L. Lutsen, D. Vanderzande, J. Manca, A. Senes, A. Bonfiglio, *Sol. Energy Mater. Sol. Cells* **2007**, *91*, 385.
[132] J. Zhao, A. Swinnen, G. Van Assche, J. Manca, D. Vanderzande, B. Van Mele, *J. Phys. Chem. B* **2009**, *113*, 1587.
[133] J. Vandenbergh, B. Conings, S. Bertho, J. Kesters, D. Spoltore, S. Esiner, J. Zhao, G. Van Assche, M. M. Wienk, W. Maes, L. Lutsen, B. Van Mele, R. A. J. Janssen, J. Manca, D. J. M. Vanderzande, *Macromolecules* **2011**, *44*, 8470.
[134] Y. Ning, L. Lv, Y. Lu, A. Tang, Y. Hu, Z. Lou, Y. Hou, *Int. J. Photoenergy* **2014**, *2014*, 1.
[135] J. Kesters, P. Verstappen, J. Raymakers, W. Vanormelingen, J. Drijkoningen, J. D'Haen, J. Manca, L. Lutsen, D. Vanderzande, W. Maes, *Chem. Mater.* **2015**, *27*, 1332.
[136] N. Shin, H.-J. Yun, Y. Yoon, H. J. Son, S.-Y. Ju, S.-K. Kwon, B. Kim, Y.-H. Kim, *Macromolecules* **2015**, *48*, 3890.
[137] W. R. Mateker, J. D. Douglas, C. Cabanetos, I. T. Sachs-Quintana, J. A. Bartelt, E. T. Hoke, A. El Labban, P. M. Beaujuge, J. M. J. Fréchet, M. D. McGehee, *Energy Environ. Sci.* **2013**, *6*, 2529.
[138] I. T. Sachs-Quintana, T. Heumüller, W. R. Mateker, D. E. Orozco, R. Cheacharoen, S. Sweetnam, C. J. Brabec, M. D. McGehee, *Adv. Funct. Mater.* **2014**, *24*, 3978.
[139] O. Synooka, K. R. Eberhardt, C. R. Singh, F. Hermann, G. Ecke, B. Ecker, E. Von Hauff, G. Gobsch, H. Hoppe, *Adv. Energy Mater.* **2014**, *4*, 1300981.
[140] M. Saito, I. Osaka, Y. Suzuki, K. Takimiya, T. Okabe, S. Ikeda, T. Asano, *Sci. Rep.* **2015**, *5*, 14202.
[141] S. Bertho, G. Janssen, T. J. Cleij, B. Conings, W. Moons, A. Gadisa, J. D'Haen, E. Goovaerts, L. Lutsen, J. Manca, D. Vanderzande, *Sol. Energy Mater. Sol. Cells* **2008**, *92*, 753.
[142] C. Müller, *Chem. Mater.* **2015**, *27*, 2740.
[143] S. Tokito, H. Tanaka, K. Noda, A. Okada, Y. Taga, *Appl. Phys. Lett.* **1997**, *70*, 1929.
[144] M. Hermenau, K. Leo, M. Riede, *Proc. SPIE* **2010**, *7722*, 77220K1.
[145] B. Song, Q. C. Burlingame, K. Lee, S. R. Forrest, *Adv. Energy Mater.* **2015**, *5*, 1401952.
[146] Q. Wang, Y. Luo, H. Aziz, *Appl. Phys. Lett.* **2010**, *97*, 063309.
[147] J. A. Bartelt, Z. M. Beiley, E. T. Hoke, W. R. Mateker, J. D. Douglas, B. A. Collins, J. R. Tumbleston, K. R. Graham, A. Amassian, H. Ade, J. M. J. Fréchet, M. F. Toney, M. D. McGehee, *Adv. Energy Mater.* **2013**, *3*, 364.
[148] B. Conings, S. Bertho, K. Vandewal, A. Senes, J. D'Haen, J. Manca, R. a. J. Janssen, *Appl. Phys. Lett.* **2010**, *96*, 163301.
[149] B. Watts, W. J. Belcher, L. Thomsen, H. Ade, P. C. Dastoor, *Macromolecules* **2009**, *42*, 8392.
[150] M. De Jong, D. Simons, M. Reijme, L. IJzendoorn van, A. Gon van de, M. Voigt de, H. Brongersma, R. Gymer, *Synth. Met.* **2000**, *110*, 1.
[151] S. T. Lee, Z. Q. Gao, L. S. Hung, *Appl. Phys. Lett.* **1999**, *75*, 1404.
[152] F. J. Esselink, G. Hadziioannou, *Synth. Met.* **1995**, *75*, 209.
[153] C. W. T. Bulle-Lieuwma, W. J. H. van Gennip, J. K. J. van Duren, P. Jonkheijm, R. A. J. Janssen, J. W. Niemantsverdriet, *Appl. Surf. Sci.* **2003**, *203–204*, 547.
[154] T. P. Nguyen, J. Ip, P. Jolinat, P. Destruel, *Appl. Surf. Sci.* **2001**, *172*, 75.
[155] I. Cardinaletti, J. Kesters, S. Bertho, B. Conings, F. Piersimoni, J. D'Haen, L. Lutsen, M. Nesladek, B. Van Mele, G. Van Assche, K. Vandewal, A. Salleo, D. Vanderzande, W. Maes, J. V. Manca, *J. Photonics Energy* **2014**, *4*, 040997.
[156] D. He, X. Du, W. Zhang, Z. Xiao, L. Ding, *J. Mater. Chem. A* **2013**, *1*, 4589.
[157] G. Griffini, J. D. Douglas, C. Piliego, T. W. Holcombe, S. Turri, J. M. J. Fréchet, J. L. Mynar, *Adv. Mater.* **2011**, *23*, 1660.
[158] B. J. Kim, Y. Miyamoto, B. Ma, J. M. J. Fréchet, *Adv. Funct. Mater.* **2009**, *19*, 2273.
[159] J. Kesters, S. Kudret, S. Bertho, N. Van Den Brande, M. Defour, B. Van Mele, H. Penxten, L. Lutsen, J. Manca, D. Vanderzande, W. Maes, *Org. Electron. Phys., Mater. Appl.* **2014**, *15*, 549.
[160] Z. Li, H. C. Wong, Z. Huang, H. Zhong, C. H. Tan, W. C. Tsoi, J. S. Kim, J. R. Durrant, J. T. Cabral, *Nat. Commun.* **2013**, *4*, 2227.
[161] C. Y. Chang, C. E. Wu, S. Y. Chen, C. Cui, Y. J. Cheng, C. S. Hsu, Y. L. Wang, Y. Li, *Angew. Chemie - Int. Ed.* **2011**, *50*, 9386.

[162] F. Piersimoni, G. Degutis, S. Bertho, K. Vandewal, D. Spoltore, T. Vangerven, J. Drijkoningen, M. K. Van Bael, A. Hardy, J. D'Haen, W. Maes, D. Vanderzande, M. Nesladek, J. Manca, *J. Polym. Sci. Part B Polym. Phys.* **2013**, *51*, 1209.
[163] E. F. Palermo, S. B. Darling, A. J. McNeil, *J. Mater. Chem. C* **2014**, *2*, 3401.
[164] C. H. Peters, I. T. Sachs-Quintana, W. R. Mateker, T. Heumueller, J. Rivnay, R. Noriega, Z. M. Beiley, E. T. Hoke, A. Salleo, M. D. McGehee, *Adv. Mater.* **2012**, *24*, 663.
[165] P. H. Lee, C. C. Torng, Y. C. Lin, *Appl. Math. Model.* **2011**, *35*, 4023.
[166] E. S. R. Bovill, J. Griffin, T. Wang, J. W. Kingsley, H. Yi, A. Iraqi, A. R. Buckley, D. G. Lidzey, *Appl. Phys. Lett.* **2013**, *102*, 183303.
[167] E. Voroshazi, I. Cardinaletti, T. Conard, B. P. Rand, *Adv. Energy Mater.* **2014**, *4*, 1400848.
[168] T. M. Clarke, C. Lungenschmied, J. Peet, N. Drolet, K. Sunahara, A. Furube, A. J. Mozer, *Adv. Energy Mater.* **2013**, *3*, 1473.
[169] D. Gedefaw, M. Tessarolo, M. Prosa, M. Bolognesi, P. Henriksson, W. Zhuang, M. Seri, M. Muccini, M. R. Andersson, *Sol. Energy Mater. Sol. Cells* **2016**, *144*, 150.
[170] Q. Burlingame, X. Tong, J. Hankett, M. Slootsky, S. R. Forrest, *Energy Environ. Sci.* **2015**, *8*, 1005.
[171] A. Distler, T. Sauermann, H.-J. Egelhaaf, S. Rodman, D. Waller, K.-S. Cheon, M. Lee, D. M. Guldi, *Adv. Energy Mater.* **2014**, *4*, 1300693.
[172] T. Heumueller, W. R. Mateker, A. Distler, U. F. Fritze, R. Cheacharoen, W. H. Nguyen, M. Biele, M. Salvador, M. von Delius, H.-J. Egelhaaf, M. D. McGehee, C. J. Brabec, *Energy Environ. Sci.* **2015**, *9*, 247.
[173] X. Tong, N. Wang, M. Slootsky, J. Yu, S. R. Forrest, *Sol. Energy Mater. Sol. Cells* **2013**, *118*, 116.
[174] N. Wang, X. Tong, Q. Burlingame, J. Yu, S. R. Forrest, *Sol. Energy Mater. Sol. Cells* **2014**, *125*, 170.
[175] P. Zhou, A. M. Rao, K. A. Wang, J. D. Robertson, C. Eloi, M. S. Meier, S. L. Ren, X. X. Bi, P. C. Eklund, M. S. Dresselhaus, *Appl. Phys. Lett.* **1992**, *60*, 2871.
[176] A. M. Rao, P. Zhou, K. Wang, G. T. Hager, J. M. Holden, Y. Wang, W. Lee, X. Bi, P. C. Eklund, D. S. Cornett, M. A. Duncan, J. Amster, *Science* **1993**, *259*, 955.
[177] N. Matsuzawa, M. Ata, D. a. Dixon, G. Fitzgerald, *J. Phys. Chem.* **1994**, *98*, 2555.
[178] P. C. Eklund, A. M. Rao, P. Zhou, Y. Wang, J. M. Holden, *Thin Solid Films* **1995**, *257*, 185.
[179] A. Dzwilewski, T. Wågberg, L. Edman, *Phys. Rev. B - Condens. Matter Mater. Phys.* **2007**, *75*, 1.
[180] A. Dzwilewski, T. Wågberg, L. Edman, *J. Am. Chem. Soc.* **2009**, *131*, 4006.
[181] R. a. Street, A. Krakaris, S. R. Cowan, *Adv. Funct. Mater.* **2012**, *22*, 4608.
[182] R. Street, J. Northrup, B. Krusor, *Phys. Rev. B* **2012**, *85*, 205211.
[183] R. a. Street, D. M. Davies, *Appl. Phys. Lett.* **2013**, *102*, 2013.
[184] J. Kong, S. Song, M. Yoo, G. Y. Lee, O. Kwon, J. K. Park, H. Back, G. Kim, S. H. Lee, H. Suh, K. Lee, *Nat. Commun.* **2014**, *5*, 5688.
[185] M. M. Mandoc, F. B. Kooistra, J. C. Hummelen, B. de Boer, P. W. M. Blom, *Appl. Phys. Lett.* **2007**, *91*, 263505.
[186] S. R. Cowan, W. L. Leong, N. Banerji, G. Dennler, A. J. Heeger, *Adv. Funct. Mater.* **2011**, *21*, 3083.
[187] J. C. Blakesley, D. Neher, *Phys. Rev. B* **2011**, *84*, 075210.
[188] G. Garcia-Belmonte, P. P. Boix, J. Bisquert, M. Lenes, H. J. Bolink, A. La Rosa, S. Filippone, N. Martín, *J. Phys. Chem. Lett.* **2010**, *1*, 2566.
[189] T. Heumueller, T. M. Burke, W. R. Mateker, I. T. Sachs-Quintana, K. Vandewal, C. J. Brabec, M. D. McGehee, *Adv. Energy Mater.* **2015**, *5*, 1500111.
[190] C. Bracher, H. Yi, N. W. Scarratt, R. Masters, A. J. Pearson, C. Rodenburg, A. Iraqi, D. G. Lidzey, *Org. Electron.* **2015**, *27*, 266.
[191] J. Kuwabara, T. Yasuda, N. Takase, T. Kanbara, *ACS Appl. Mater. Interfaces* **2015**, acsami.5b09482.
[192] G. Wantz, L. Derue, O. Dautel, A. Rivaton, P. Hudhomme, C. Dagron-Lartigau, *Polym. Int.* **2014**, *63*, 1346.
[193] D. K. Susarova, N. P. Piven, A. V. Akkuratov, L. A. Frolova, M. S. Polinskaya, S. A. Ponomarenko, S. D. Babenko, P. A. Troshin, *Chem. Commun.* **2015**, *51*, 2239.
[194] N. Björklund, J.-O. Lill, J. Rajander, R. Österbacka, S. Tierney, M. Heeney, I. McCulloch, M. Cölle, *Org. Electron.* **2009**, *10*, 215.
[195] R. S. Ashraf, B. C. Schroeder, H. A. Bronstein, Z. Huang, S. Thomas, R. J. Kline, C. J. Brabec, P. Rannou, T. D. Anthopoulos, J. R. Durrant, I. McCulloch, *Adv. Mater.* **2013**, *25*, 2029.
[196] K. T. Nielsen, K. Bechgaard, F. C. Krebs, *Synthesis (Stuttg).* **2006**, *10*, 1639.
[197] R. F. Salzman, J. Xue, B. P. Rand, A. Alexander, M. E. Thompson, S. R. Forrest, *Org. Electron.* **2005**, *6*, 242.
[198] M. Hermenau, M. Riede, K. Leo, in *Stab. Degrad. Org. Polym. Sol. Cells* (Ed.: F. C. Krebs), John Wiley And Sons, Chichester, UK, **2012**, pp. 109–142.
[199] R. Franke, B. Maennig, A. Petrich, M. Pfeiffer, *Sol. Energy Mater. Sol. Cells* **2008**, *92*, 732.
[200] S. Schmidbauer, A. Hohenleutner, B. König, *Adv. Mater.* **2013**, *25*, 2114.